Rapid Detection of Trace Metal Ions on Microfluidic Platforms using Gold Nanoparticle Sensors

Presented by

Guowei Zhong

Department of Civil Engineering and Applied Mechanics

McGill University, Montreal

July 2013

A thesis submitted to McGill University in partial fulfillment of the requirements of the degree of Master of Science

ABSTRACT

The presence of metal ions, especially heavy metals, in various waters at elevated levels can pose a high risk to the environment and human health. Drinking water is one of the major sources that contributes to the daily intake of heavy metals by humans, and thus a rapid, low-cost and sensitive method for detection of heavy metal content in water is desirable. The goals of this study are to develop a chemical method for rapid testing of lead (Pb^{II}) ion in water solutions and to incorporate the method into a portable device for potential onsite applications. First, a rapid and sensitive colorimetric method for lead detection has been developed in this study by utilizing the unique optical properties and surface chemistry of gold nanoparticles (GNPs) and glutathione (GSH), which is a peptide used for lead recognition. In the reaction, GSH molecules serve as linkers to coordinate with both Pb^{II} and GNPs so as to aggregate the GNPs and thereby change the colour of the assay solution. The colour changes as measured by absorbance at selected wavelengths using UV-Vis spectrometry are proportional to the levels of Pb^{II} in aqueous samples, and thus quantification of Pb^{II} can be realized. As the reaction is based on label-free GNPs, no pre-modification is required. The limit of detection (LOD) of 6.0 ppb achieved by the method is lower than the maximum acceptable Pb^{II} concentrations (10 -15 ppb) in drinking water, indicating its high sensitivity and potential applicability in

drinking water testing. The high selectivity for Pb^{II} against 10 metal ions has been demonstrated, and several masking agents were evaluated for their effectiveness in reducing potential inferences for an additional four metals. Second, a polydimethylsiloxane (PDMS) microfluidic chip was fabricated and coupled with a portable optical reader specifically designed for GNP probes. This device was first tested for detection of aluminum (Al^{III}) as a model compound by GNP probes to examine the compatibility of the microfluidic chip with the GNP probes and the sensitivity to the corresponding colour changes of the GNPs. It showed an LOD (1.2 ppm) comparable with that of UV-Vis Spectrometry (1.3 ppm) and operations were simple since only pipetting was required. The prominent feature of the device is that PDMS microfluidic chips are disposable and can be redesigned for other assays as well, such that the label-free GNP probes developed in this study for Pb^{II} detection can be possibly integrated in those microfluidic chips in the near future. The use of LED array light sources with controllable wavelengths is another feature to enable multi-analyte capability, which could be examined in the near future.

RÉSUMÉ

La présence d'ions métalliques en particulier les métaux lourds dans différents types d'eau à des niveaux élevés peut présenter un risque important pour l'environnement et la santé humaine. L'eau potable est l'une des principales sources qui contribuent à l'apport quotidien en métaux lourds chez l'humain, et donc une méthode rapide, peu coûteuse et sensible à la détection des métaux lourds dans l'eau est en grande demande. Les objectifs de cette étude est de développer une méthode chimique pour un dépistage rapide d'ion de plomb (Pb^{II}) en phase aqueuse et d'intégrer la méthode dans un dispositif portable à des fins d'applications potentielles sur place. Premièrement, une méthode colorimétrique rapide et sensible à la détection de plomb a été développée dans cette étude en utilisant les propriétés optiques uniques et la chimie de surface des nanoparticules d'or (GNPs) et le glutathion (GSH), qui est un peptide utilisé pour la reconnaissance de plomb. En réaction, les molécules de GSH servent de relieurs à fin de coordonner avec le Pb^{II} ainsi que le GNPs de manière à regrouper les sondes GNPs et ainsi changer la couleur du dosage. Les changements de couleur mesurée par absorption à des longueurs d'onde sélectionnées en utilisant la spectrométrie d'UV-Vis sont proportionnels au niveau du Pb^{II} dans des échantillons aqueux, permettant ainsi la quantification de Pb^{II}. Comme la réaction est basée sur l'utilisation des GNPs non-libellés, pas de pré-modification est requise. La limite de détection (LOD) de 6,0 ppb réalisée par la méthode est inférieure aux concentrations maximales de Pb^{II} acceptable (10 à 15 ppb) dans l'eau potable, ce qui indique sa haute sensibilité et applicabilité potentielle en analyse d'eau potable. Une haute sélectivité pour le Pb^{II} contre 10 ions

métalliques a été démontrée, et plusieurs agents masquant ont été évalués pour leur efficacité dans la réduction des interférences potentielles pour quatre autres métaux. Deuxièmement, une puce microfluidique en polydiméthylsiloxane (PDMS) a été fabriqué et couplé à un lecteur optique portable spécialement conçu pour les sondes de GNPs. Cet appareil a été d'abord testé pour la détection de l'aluminium (Al^{III}) comme composé modèle, par des sondes de GNPs à fin d'examiner la compatibilité de la puce microfluidique avec les sondes de GNPs et la sensibilité aux changements de couleur correspondante du GNPs. Elle a démontré une LOD comparable (1,2 ppm) à celui de la spectrométrie UV-Vis (1,3 ppm) et les opérations étaient simples puisque seulement le pipetage était nécessaire. L'aspect remarquable du dispositif est que les puces microfluidiques de PDMS sont jetables et peuvent être reformulées pour d'autres dosages ainsi, de sorte que les sondes de GNPs non-libellées développées dans cette étude pour la détection de Pb^{II} peuvent être éventuellement intégrés dans des études futures. L'utilisation des sources de lumière à faisceau LED aux longueurs d'onde contrôlables est une autre caractéristique permettant une capacité multi-analyte, qui pourrait être examinée dans un proche avenir.

CONTRIBUTION OF AUTHORS

The thesis consists of a general introduction, a manuscript of a literature review, a manuscript of a chemical assay and a preliminary result on a microfluidic device prototype. Chapter 1 is the general introduction which was written by the candidate and revised by his supervisor Dr. Jinxia Liu. Chapter 2, the manuscript of the literature review on the microfluidic sensing systems for detection of heavy metal ions in water, was co-authored by the candidate, his supervisor Dr. Jinxia Liu and co-supervisor Dr. Xinyu Liu at the department of Mechanical Engineering of McGill University. Chapter 3, the manuscript on detection of lead by GNPs was co-authored by the candidate and his supervisor Dr. Jinxia Liu and Dr. Xinyu Liu. Chapter 4, the preliminary study on the microfluidic device integrated with the portable optical reader for the detection of aluminum by GNPs, was written by the candidate and edited by his supervisors Dr. Jinxia Liu and Dr. Xinyu Liu. The idea of using GNPs for detection of heavy metals was from Dr. Jinxia Liu and the development of an optical reader for metal detection was done by Dr. Xinyu Liu and his group in McGill University, including the PhD candidate Chen Zhao and the undergraduate student Da-Eun Kim. The protocol for the detection of lead using label-free GNPs was designed and developed by the candidate. The candidate fulfilled his obligation for laboratory experiments, data collection/analysis, data interpretations and writing of the two manuscripts under the supervision of Dr. Jinxia Liu and Dr. Xinyu Liu.

ACKNOWLEDGEMENTS

I dedicated this thesis foremost to my supervisor Dr. Jinxia Liu. You are such a nice person and always trusts and guides me with all patience. It was such an honor to work with you because I was inspired by your wealth of knowledge and richness of experience. I feel lucky and would like to share with anyone else that I have met the best supervisor in the world. Secondly, I would like to thank Dr. Xinyu Liu, whose work demonstrated to me the state-of-the-art and promising applications of microfluidics. I want to thank you both for encouraging me to accomplish the goals and provided me funding generously. I also owe a debt of gratitude to Professor Ronald Gehr who became my initial academic supervisor in McGill University.

In addition, it is with immense gratitude that I acknowledge the support and help of my parents, who gave me the opportunity of an education from the best university and always supported me unconditionally throughout my life. You really mean everything to me! Without you and your support, I would have given up my dream.

In addition, I want to thank all my friends in Montreal, especially Mauhamad Shamee Jauffur and Jing Li for their helps on this study.

Thank you so much! May you all realise your dreams and be happy every day!

Table of Contents

LIST OF TABLES

LIST OF FIGURES

CHAPTER I INTRODUCTION

1.1 Problem statement

Some heavy metals are among the most hazardous chemical contaminants for humans and the environment due to their toxic and non-degradable nature[1]. The most common adverse effects on humans include developmental neurotoxicity, neurodegenerative effects, and cardiovascular effects, etc.[2] To minimize human exposure to heavy metal pollutants, Health Canada sets strict guidelines on a number of heavy metals (10 ppb or lower for each metal) for Canadian drinking water[3] and similar guidelines and regulations are in place in many other countries as well as by the World Health Organization (WHO)[1]. For instance, the upper permissible limits for arsenic and lead are 10 ppb in *Canadian Guidelines for Drinking Water* [3] as well as *WHO Guidelines for Drinking Water Quality*[1]. The ability to detect and quantify heavy metals with high sensitivity and selectivity is among the first steps to implement those regulations.

Heavy metals in environmental samples (water, soil, sediments, etc.) are typically detected and quantified using atomic absorption spectrometry (AAS), inductively-coupled plasma atomic emission spectrometry (ICP-AES), or inductively-coupled plasma mass spectrometry (ICP-MS). These analytical methods have proven to be highly sensitive and selective, and are capable of measuring very low levels of metal ions (e.g. 1 ppb or lower using AAS for lead

detection)[4]. Yet, these techniques require highly sophisticated analytical equipment and costly consumables[5], and must be operated by highly skilled analysts. These techniques cannot be used onsite because the required equipment is bulky and immobile[6]. With ever increasing demands for better quality of life, there is a great need of portable sensing devices for onsite heavy metal detection in water. Such devices need to be simple and of low cost to operate, yet with sufficient sensitivity and even multi-target capability.

Aside from those highly sophisticated instruments, detection techniques such as colorimetry, fluorimetry, and voltammetry that use equipment of small footprints and high portability have been explored. In the past few years, nanomaterials have been shown promising on improving detection limits as well as miniaturization of sensing devices[1, 6]. In particular, gold nanoparticles (GNPs) have shown great promise for heavy metal detection as well as many other applications, owing to its special optical and surface chemical properties, such as surface plasmon resonance (SPR).

SPR is a non-linear optical property originating from the absorbance of the incident light (electromagnetic radiation) by the collective oscillation of the conduction electrons at the surface under irradiation of light[7]. In general, a SPR peak of GNPs is highly sensitive to the dielectric (refractive index) nature of the immediate medium of GNPs. When there is any small change on the GNP

surface or its immediate surroundings (surface modification, aggregation, etc.), the frequency of the peak will change and GNPs can produce detectable colour changes[8]. This property allows GNPs to be an excellent colorimetric sensor. For instance, GNPs have been used as biosensors for adenosine[9], peptide[10], DNA[8] as well as heavy-metal sensors[11]. Another highly useful property of GNPs is that GNPs can be easily functionalized by a thiol group through covalent bonds[12], and various thiol-containing molecules can be attached to GNP surfaces[13]. The functionalization of GNPs alters their stability, functionality and biocompatibility[14].

In general, there are three strategies for utilizing functionalized GNPs for detection of heavy metals. The first strategy is to utilize the modified (or functionalized) GNPs as probes after a series of processes including GNP synthesis, modification, purification or extraction. This approach has been used for arsenic[15], mercury[16] and lead detection[17]. It has shown high sensitivity and strong capability against interferences from other non-target metal ions, yet there are several drawbacks. For instance, the approach requires sequential extraction of the modified GNPs. Moreover, the short half-life of the thiolated GNPs, caused by rapid decay of the thiol-containing reagent used for functionalization[18], greatly limits onsite applications because it is difficult to maintain the functionality of the modified GNPs. The second strategy is to combine GNP synthesis with modification into one step to directly synthesize

thiolate-capped GNPs, thus eliminating the purification step. In this approach, thiol-containing reagents function as a reducing agent during the synthesis of GNPs, and excess thiol-containing reagents will remain in the solution to cap and protect the GNPs[19]. However, this approach still creates thiolated GNPs of short shelf-life which is not desired for onsite applications.

The third strategy, using label-free (or non-functionalized) GNPs for heavy metal detection, was introduced by Li, et al. [20]. The researchers designed a special peptide, which contained three thiol functional groups from a tricysteine structure for specifically recognizing zinc as well as the GNPs. The thiol groups coordinate with either GNPs when zinc is absent, or with zinc when both GNPs and zinc are present due to the higher affinity between zinc and the peptide. When zinc is absent, an arginine residue of the peptide helps to aggregate the GNPs by neutralizing GNP surface charges, and consequentially, the aggregation of GNPs causes detectable colour changes. When zinc is present, the GNPs will remain unaggregated, as the peptide complexes with zinc, and will show the original colour. The advantage of this approach is that neither purification process nor strict preservation conditions for GNPs are required. A similar approach was further explored by Xia, et al. [5] for arsenic determination. In above-mentioned studies, citrate-capped GNPs are normally used, and these GNPs are very stable and can be preserved at room temperature. Due to the

apparent advantages, citrate-capped GNPs have been used throughout the experiments as described in the thesis. More specifically, glutathione (GSH), a thiol-containing peptide, has been used for functionalizing the GNPs, as well as for recognizing aqueous lead ions. Both processes occur at the same time, as the thiol group are be favoured by the GNPs and the carboxylic groups of glutathione molecules are used for lead recognition.

Additional to the application of the GNP sensors, a microfluidic platform has been coupled to realize the analysis independent from the traditional bench-top lab equipment. Lab-on-a-chip or micro total analysis systems (μTAS) that are based on microfluidics have attracted much attention over the past decade. As the name suggests, the microfluidics have the premise of manipulating and analyzing fluids in microliter sizes[21]. It is featured by low consumption of reagents and samples, which can be critical in biological, medical and environmental applications. A large variety of techniques have been developed for the fabrication of microfluidic devices[22]. The most suitable fabrication technique depends on several factors such as the material properties, the size limit of the fluid channel, or the cost. The techniques for processing silicon and glass were once among the most popular ones for fabrication of microfluidic devices, as they were well-established and could be borrowed directly from the semiconductor industry at an early stage of development of microfluidic devices[23]. Yet, they are

limited by several disadvantages, for instance, high cost for glass processing or lack of transparency for the silicon-based devices. Later, Whitesides and coworkers[24] described a famous technique – soft lithography, which uses polydimethylsiloxane (PDMS) as the material for fabrication of microfluidic devices. PDMS is advantageous due to its high transparency, air and water permeability and ease of fabrication[25]. The high transparency of PDMS makes it an excellent material for colorimetric/spectrometric detection. It can be easily integrated with optical elements such as photomultiplier tubes (PMT) and light-emitting diodes (LED) to make a compact device which shares excellent traits such as low energy consumption and small profiles. Microfluidic devices made of PDMS have been widely used in environmental fields, capable of determining environmental indicators such as phytoplankton[26], mycobacteria[27], urea[28], aerosol particles[29], heavy metals[30], etc.

In addition, through integration of other bio- or chemo- sensors into PDMS microfluidic devices, detection limits can be greatly improved[30a, 31]. It has been demonstrated that coupling of GNPs into a PDMS device with integrated optical elements yields the capability for determining concentrations of heavy metals, even with a simple design[32]. A device with more sophisticated design for the detection of several heavy metal species in parallel has also been demonstrated

by using several bio-sensors[33]. Therefore, PDMS is used as the material for microfluidic device fabrication throughout the studies as described in the thesis.

1.2 Objectives

This research aims at developing a microfluidic platform for detection of trace metal ions using GNP sensors. The device using GNPs is expected to have high sensitivity and selectivity, and a multi-analyte capability. The specific objectives are:

1) To develop an assay involving label-free GNPs for lead detection in aqueous solutions with the sensitivity to meet the criteria for drinking water;
2) To optimize the assay to minimize the impact from potential interfering ions that are possibly present in environmental water samples;
3) To design and fabricate a PDMS microfluidic chip with considerations for multi-analyte detection, and to integrate it with an optical reader designed specifically for SPR of GNPs;
4) To optimize the operation parameters of the device for sensitive detection of aluminum as a model compound in water.

1.3 Scope and Approach

The GNPs were fabricated based on the classic Turkevich – Frens method[34] with the protocol modified from Liu and Lu [35].

In this thesis, the label-free GNPs, which will be modified by GSH molecules during the assay, serve as the probes that coordinate with the target lead ion (Pb^{II}) due to its high affinity and as the reporters that are detectable via UV-Vis spectrometry owing to colour changes during their aggregation.

The sizes of GNPs were analyzed by transmittance electronic microscope (TEM) (Tecnai GF20 which equipped with Gatan Ultrascan 4000 4k x 4k CCD Camera System Model 895 and EDAX Genesis EDS and operated at 200 keV). The images were analyzed by ImageJ.

UV-Vis spectrometry analyses were performed using SpectraMax M5, under scanning and kinetic modes. Absorbance curves were reconstructed using Microsoft Excel.

The PDMS chip was designed in AutoCAD® and fabricated using a mold which was manufactured by using a Universal Laser Systems VLS2.30.

CHAPTER II LITERATURE REVIEW: MICROFLUIDIC SENSING SYSTEMS FOR DETECTION OF HEAVY METAL IONS IN WATER

(A draft prepared for submission to *Trends in Analytical Chemistry)*

2.1 Abstract

Microfluidic devices have gained growing popularity for applications in water monitoring in the past decade. It is believed that these devices are capable of overcoming some of the drawbacks of traditional analytical methods such as high cost and bulkiness. Microfluidic devices share the advantages of ease of fabrication, low cost, portability and capable of onsite applications. They provide quantitative determination of heavy metal ions by incorporating bio-, chemo-, or electrochemical sensors. These sensors are highly suitable for microfluidic devices, as they give off signals for either optical or electrochemical detection. Besides, these devices are made from inexpensive materials and batch fabricated, which ensures the low cost. In this chapter, the working mechanisms of the sensors will be introduced; detailed design and the performances of the corresponding devices are to be discussed. Furthermore, the future trends of using microfluidic devices for heavy metal detection, including integration of nano-materials, application of paper-based devices and complex integrated

systems with built-in sample preparation functionality, signal processing and data communication, are suggested.

2.2 Introduction

2.2.1 Heavy metal contamination

Heavy metal pollution can be attributed to both anthropogenic sources (including fossil fuel and coal combustion, industrial effluents, solid waste disposal, fertilizers, mining and metal processing, etc.) and natural sources[36]. Some heavy metals (eg., arsenic, lead and mercury) are highly toxic and carcinogenic, posing a high risk to the environment and human health. To minimize human exposure to heavy metal pollutants, WHO and many countries in the world set strict guidelines on levels of heavy metals allowed in drinking water[3]. For instance, the upper permissible limits for arsenic and lead are 10 ppb in the *WHO Guidelines for Drinking Water Quality*[1]. The ability to detect and quantify heavy metals with high sensitivity and selectivity is among the first steps to implement those regulations.

Major laboratory techniques used for heavy metal detection and quantification are atomic absorption spectrometry (AAS), inductively-coupled plasma atomic emission spectrometry (ICP-AES), or inductively-coupled plasma mass spectrometry (ICP-MS). These are robust techniques suitable for a wide

range of heavy metals and they can achieve high precision and low detection limits[37]. Arsenic, for instance, can be detected in an environmental sample to lower parts per billion (ppb) by ICP-AES[4]. The use of these sophisticated techniques is limited to only highly trained analysts in laboratories. There is a need for analytical devices that are suitable for rapid field testing, or for point-of-use. New techniques such as microfluidic devices with portable, robust, autonomous and accurate characteristics are attracting tremendous attention in recent years[38]. There has been rapid advancement in detecting heavy metal ions in water samples.

2.2.2 Microfluidics and sensing systems

Microfluidic devices, capable of small-scale manipulation of fluids, can be used for medical diagnostics as well as detection of environmental pollutants. Such miniaturization has led to features such as portability, low sample and reagent consumption, small sample size, low energy consumption, rapid detection, and very importantly, low cost to build and operate such devices. There are two general trends of device designs. One is to fabricate a fully-integrated analytical device for onsite analysis, regardless whether for medical or environmental applications, and this has led to the concept of micro-total analysis systems (μTASs)[39]. The micro-total analysis system (μTAS), or so-called “lab-on-a-chip”,

is a system of microfluidic components that incorporates all necessary steps from sample pretreatment, dilution, calibration, separation, derivatization, and ultimate detection[40]. The other trend is to design a simple low-cost system, such as a paper-based device which is of high portability and low-cost, to enable simple and rapid testing for either onsite applications or daily use.

More details on the microfluidic systems designed for environmental analysis and for ionic species detection are available in the literature[41]. Articles on specific topics such as electrochemical sensors[38b] and conductometric microbiosensors[42] for water monitoring are available. A mini review that compiles research on biosensors for heavy metal determination is also available[43], but the applications of the sensors reviewed in that study require the aid of traditional instruments (e.g. UV-Vis spectrometry). Nano-structured sensors for heavy metals are also reviewed by Li et al.[44]. A comprehensive review on microfluidic devices coupled with different types of sensors for heavy metal detection is, however, lacking.

Generally, categorization of microfluidic devices is based on the signal acquisition methods or the detection methods[38a, 45]. Signal acquisition usually consists of optical measurement and/or electrochemical measurement by sensors. As the sensors are the key components influencing the performance of

the microfluidic devices, the focus can also be placed on the improvement of different bio-, chemo- and electrochemical sensors themselves.

Therefore, we believe a review of the current advances in the sensors used in microfluidic devices for measuring heavy metals in environmental samples can further promote the use of microfluidic technology in environmental analysis. We organize the information based on the nature (materials and mechanisms) of the sensors (Figure 2.1), and three major types of sensors, bio-, chemo- and electrochemical sensors, will be introduced. The review discusses fundamental working mechanisms of the sensors, methods of integration into microfluidic devices, sensor performance, as well as signal acquisition methods. The advantages and drawbacks of these sensors are also compared and future research directions for heavy metal detection on microfluidic platforms are suggested.

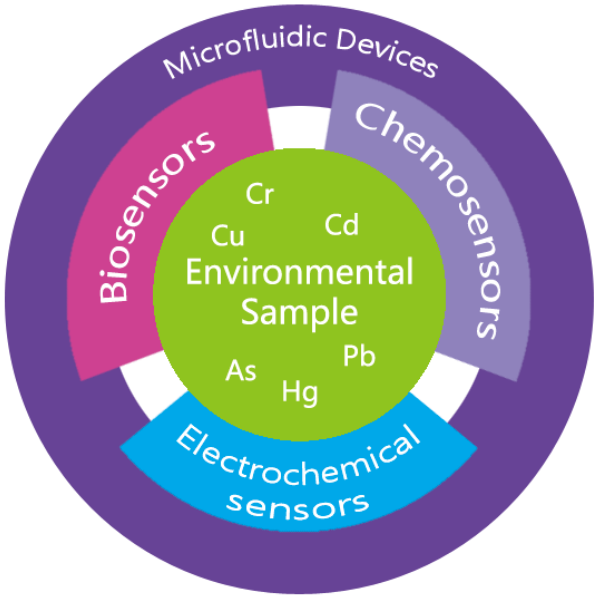

Figure 2.1: Various types of sensors that can be integrated into microfluidic devices for heavy metal detection

2.3 Heavy metal monitoring sensors

2.3.1 Bio-sensor

2.3.1.1 Nucleotide-based

Monitoring heavy metal ions in aqueous solutions by nucleotide-based probes has been recently developed. These probes are designed to engage complexation reactions with target metal ions to either produce fluorescent or colorimetric signals from the nucleotides[6, 32, 46], and/or to influence activities of enzyme DNA[30a, 47]. Most of these sensors or probes that have been integrated into microfluidic platforms are for Pb and mercury (Hg) detection as summarized in Table 2.1.

Table 2.1: Performance and characteristics of microfluidic systems with nucleotide-based sensors for heavy metal detection

Target	LOD	Detection Range	Advantages	Limitations	Comment	Ref.
Hg^{II}	Not mentioned	5 µM - 100 µM (1 – 20 ppm)	Selective for Pb^{II}, Cd^{II}, Cu^{II}, Mn^{II}, Zn^{II}	Low sensitivity	Use of labeled GNP	*32*
Hg^{II}	Not mentioned	6.25 – 100 µM (1.25 – 20 ppm)	Selective for Zn^{II}, Co^{2+}, Mn^{II}, Cu^{II}, Pb^{II}	Low sensitivity	Droplet manipulation (Small volume)	*6*
Hg^{II}	3 ppb	Not provided	Good selectivity for Fe^{III},Cd^{II},Pb^{II},Cu^{II},Ca^{II}	PAGE* and CE** required	Sensitive but not portable	*46*
Pb^{II}	11 nM (2.3ppb)	0.1 – 100 µM (20.7 ppb – 20.7 ppm)	Easy to detect different targets by changing the enzyme DNA	Fluorescence microscopy, high voltage power source required	Verified by certified reference material	*30a*
Pb^{II}	2.1 ppt (10 pM)	6.2 ppt – 207 ppb (30 pM – 1 µM)	Extremely high sensitivity, multi-analyte	Long incubation time, washing; peripheral equipment required	3D paper-based, applied for river water	*48*
Hg^{II}	40 ppt (0.2 nM)	0.1 – 200 ppb (500 pM – 1 µM)				

* polyacrylamide gel electrophoresis

**Capillary electrophoresis

Ono and Togashi [49] developed an oligonucleotide-based sensor for Hg^{II} in aqueous solutions based on the observation that Hg^{II} can bridge pairing of thymine-thymine base pairs (T-Hg^{II}-T) on a DNA sequence to form a thermally stable duplex. The stability of the duplexes was much higher than the duplexes formed between other metal ions (such as Cu^{II}, Mn^{II}, Pb^{II}, Cd^{II}) with a T-T pair, and thus could be used for detecting Hg^{II} with high selectivity. Such a DNA sequence as a Hg^{II} sensor could be labeled by a fluorophore and a quencher[49] to allow for fluorescence detection. The fluorescence signal was either activated or

quenched by the binding of Hg^{II} due to the deformation of the molecular structure of the enzyme DNA sequence.

Integration of such an Hg^{II} sensor into microfluidic platforms was realized by He, et al. [32], where GNPs were used as a colorimetric probe and detection range of 1 – 20 ppm was reported. The device was made of PDMS, which is a material very suitable for the fabrication of colorimetric microfluidic devices, attributed to its highly transparent nature[50]. Anran, et al. [6] developed a microfluidic device for Hg^{II} detection based on a similar working mechanism by utilizing a single strand of DNA sequence in the presence of Hg^{II} to form internal T-Hg^{II}-T pairs. A special polymer-based dye was used to bind to T-Hg-T structures by electrostatic forces to enable colorimetric detection, and the detection limit was about 1.25 ppm (6.25 μM). The device also incorporated droplet manipulation driven by electrostatic forces, which assisted transportation and mixing enhancement of reagents and the sample to greatly reduce the reaction volume to a few milliliters. Such design was the key to the portability of the device for potential onsite applications. Yuan, et al. [46] developed a more sensitive microfluidic device for Hg^{II} based on a similar working mechanism. A DNA sequence without internal T-Hg^{II}-T pairs would be digested by a specific enzyme, but those with T-Hg^{II}-T structure would not be digested and therefore would be detectable on polyacrylamide gel electrophoresis (PAGE). The device

was able to measure Hg^{II} as low as 3 ppb in aqueous solutions, yet it was not suitable for onsite applications because of the use of non-portable PAGE equipment. Very recently, Zhang and his coworkers[48] developed a sophisticated 3D paper-based device for parallel detection of Pb^{II} and Hg^{II}. The recognition of Pb^{II} and Hg^{II} in this device was based on the formation of G-quadruplex (a 3D-structure formed between Pb^{II} and DNA sequences) and T-Hg^{II}-T duplexes, respectively. This device incorporating composite nano-materials for electrochemiluminescence (ECL) detection provided impressively high sensitivity in the lower ppt levels (Table 2.1), and also realized simultaneous multi-analyte detection.

Another category of nucleotide-based sensors utilizes enzyme DNA for heavy metal detection. Enzymes have been long considered to be proteins only, until some DNA[51] and RNA[52] were found to have catalytic capabilities which expanded the definition of enzymes and the catalytic DNA was then developed for Pb detection[53]. For instance, Pb^{II} can form a complex with a part of an enzyme DNA structure to promote the reactivity of the enzyme[43]. Chang, et al. [30a] described a microfluidic device for lead detection by a specific enzymatic reaction, in which the enzyme DNA could specifically recognize and cleave a probe of DNA sequence in the presence of Pb^{II}. As illustrated in Figure 2.2, the sensor was composed of a cleavable *substrate DNA* strand whose 5' and 3' ends were

labeled with a fluorophore (FAM) and a quencher (Dabcyl), respectively, and an *enzyme DNA* strand whose 3' end was labeled with a Dabcyl. The fluorescence of FAM was initially quenched by Dabcyl, and with the addition of Pb^{II} the *substrate DNA* was cleaved off and the fluorescence signal was turned on due to the separation of FAM and Dabcyl. This device had a detection limit as low as 2.3 ppb and high selectivity for real environmental samples were also demonstrated[30a]. Even for the complex composition in the electroplating sludge reference material, the device was able to quantify Pb^{II} with good agreement to the certified value. Additionally, similar enzyme DNA/RNA sensors have been developed for other heavy metals such as Cu^{II}, Zn^{II} and Co^{II} [54], but have not been integrated into microfluidic platforms.

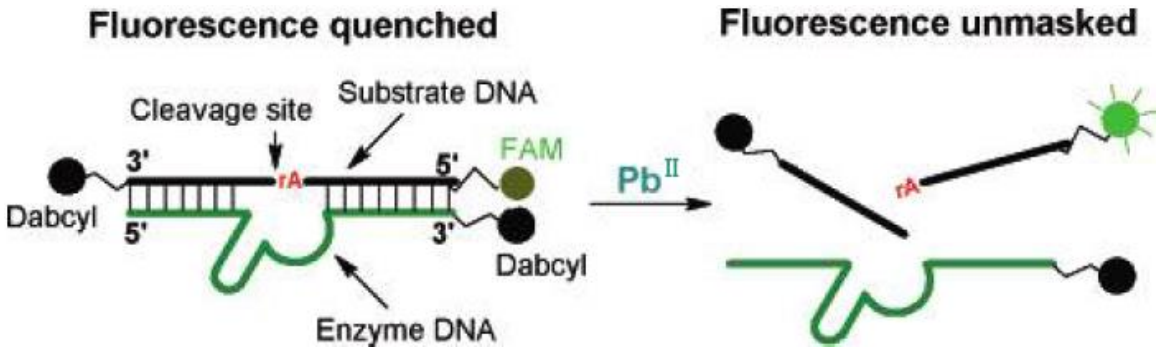

Figure 2.2: The working principle of a nucleotide-based heavy metal sensor based on enzymatic DNA.
(Source: Chang et al., 2005 with minor modifications)

2.3.1.2 Protein-based

A variety of proteins, including enzymes and antigens/antibodies, have been used as heavy metal sensors for sensitive and selective detection of heavy metals on microfluidic devices (Table 2.2). Many proteins natural to the living body such as cysteine and glutathione have a high affinity to certain heavy metal ions which enable them to function as excellent heavy metal sensors[15]. Besides, proteins with special properties can also be specifically designed and used for selective detection of certain heavy metal species[20]. Integration of such protein-based heavy metal sensors onto the microfluidic platforms has been realized and the potential for practical uses has been suggested.

Table 2.2: Performance and characteristics of microfluidic systems with protein-based sensors for heavy metal detection

Target	LOD	Detection Range	Advantages	Limitations	Comment	Ref.
Cd^{II}	0.92 ppb	0.57 – 60 ppb	Multi-analyte analysis, high sensitivity, four channels design	Pumping required	Immunoassay; GNP labled antibody	*33*
Cr^{VI}	0.04 ppb	0.03 – 0.97 ppb				
Pb^{II}	0.06 ppb	0.04 – 5.3 ppb				
Hg^{II}	Not mentioned	1 μM – 50 mM (0.2 – 10 ppm)	Extremely low cost, simple and effective	Low sensitivity	GNP probe	*55*
Hg^{II}	0.83 ppb	Not mentioned	High sensitivity	SPE procedure required	GNP probe; actual water samples tested	*56*

One example of immunoassay-based sensors coupled with a microfluidic device for heavy metals determination has been reported by Date, et al. [56], and in the study, GNP-labeled monoclonal antibodies (Ab) were able to complex with specific metal-ligand structures including Cd-EDTA, Cr-EDTA and Pb-DTPA. Antigens (Ag) were immobilized onto polymer beads in a confined region of a PDMS microfluidic chip to capture the GNP-Ab-metal-ligand complex. The advantage of such a design was that the target ions could be concentrated onto the beads to improve the signal intensity due to the high specific surface area. This device was capable of multi-analyte detection, and the simultaneous detection of Cd^{II}, Cr^{VI} and Pb^{II} was demonstrated (Table 2.2)[33]. A similar device with the same mechanism for Hg^{II} detection was also reported[56]. The capability for other heavy metals detection could be easily realized if a metal-specific antibody was made available. Furthermore, one notable feature of the devices in both studies was a handheld absorbance measurement system powered by internal batteries which could be used for onsite applications and cost-effective monitoring.

Another approach that utilized GNP probes of carboxylic modified protein to detect Hg^{II} in an assay analogous to immunoassay was described by Chao, et al. [55] (Figure 2.3). The device was constructed by several pieces of lateral flow assay (FLA) strips stacked together for lateral solution migration. As illustrated in

Figure 2.3, the conjugate strip (or pad) contained GNPs with carboxylic (COOH)-bovine serum albumin (BSA)-Biotin (the GNP probe), and the test line contained COOH-BSA species. When a liquid sample with Hg^{II} ion was wicked through the LFA strips to reach the test line, a signal was given off when Hg^{II} linked the COOH-BSA-biotin with COOH-BSA to form a sandwich-like structure. The resultant colour change in the presence of Hg^{II} could be recognized by the naked eye, which greatly simplified detection procedures and lowered cost. However, the sensitivity (Table 2.2) is yet to be improved for future practical uses.

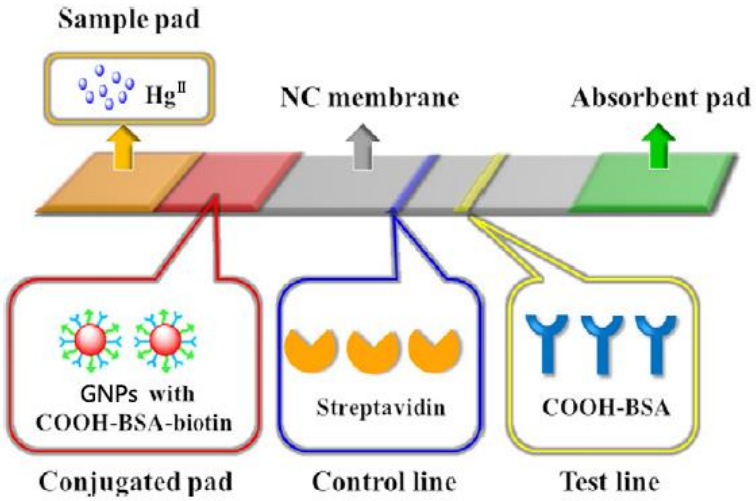

Figure 2.3: Schematic structure of a lateral flow assay with all the required components and reagents on the device
(Source: Chao, et al. [55] with minor modifications)

2.3.1.3 Whole-cell-based

Whole-cell-based sensing techniques usually utilize engineered microbes with reporter genes or spores for detection of heavy metal targets. When a specific binding event occurs between a regulatory protein and its ligand analyte (As^{III} or others), certain biochemical pathways in the engineered microbes can be activated to enable detection, usually through the expression of green fluorescence proteins[57], or the germination rate of spores can either be hindered or expedited[58]. The successful integration of such whole-cell-based bio-sensors into microfluidic devices for As^{III} detection is summarized in Table 2.3.

Table 2.3: Performance and characteristics of microfluidic systems with whole-cell-based sensors for heavy metal detection

Target	LOD	Detection Range	Advantages	Limitations	Comment	Ref.
As^{III} Anti-monite	1 µM (75 ppb)	1 µM – 5 mM 75 ppb – 375 ppm	Selective to As^{III}	Bulky equipment; not sensitive	Fluorimetric	*59*
As^{III}	10 ppb	10 ppb – 1 ppm			Fluorimetric	*57*
As^{III}	0.25 µM (18.3 ppb)	0.25 µM – 1 µM (18.3 ppb – 75 ppb)	High throughput array; autonomous system with photo sensor; processor integrated; relatively low detection limit	Complex system setup	Fluorimetric	*60*
As^{III} Zn^{II}	7.5 ppb (0.1 µM) 6.5 ppb (0.1 µM)	Up to 0.1 mM (Up to 7.5 ppm) 65 ppb – 6.5 ppm (1 µM – 100 µM)	Ease of preservation, transportation, potential of onsite application.	Not tested in microfluidic device	Chemiluminescence; Fluorescence	*61*

The protein species that has been often used as reporter cells is a nonpathogenic strain of engineered *Escherichia coli* with green fluorescence proteins (GFP)[62]. Studies have shown that when As^{III} was present in a solution, the defense system of the bacteria would be activated by a sensory protein (ArsR) and a series of genes would work together to pump out the As^{III} from the cytoplasm to protect the bacteria themselves from arsenic poisoning. When this event was coupled with the genes for GFP, the expression of GFP was triggered consequentially (Figure 2.4)[57]. Because the intensity of the fluorescence signal was proportional to the concentration of the inducer (As^{III}), quantitative measurement of As^{III} could be realized. Successful integration into microfluidic devices of such whole-cell-based sensors, based on GFP expression, has been reported[57, 59]. In addition to the use of the whole-cell sensors in the study by Rothert, et al. [59], the authors designed a compact disk (CD)-like structure that used centrifugal forces for valve controlling, reagent transport and mixing in their device. In this structure, six parallel test zones were available for high throughput and multi-analyte analyses and the authors claimed that by minimizing the sample/reagent loading area and the distance between each functional area, a higher throughput design with ten parallel test zones could be realized. A broad dynamic range from 75 ppb – 375 ppm was reported, though the detection limit was not low enough to meet the U.S. Environmental Protection Agency (U.S.

EPA) drinking water standard[63]. In addition, the motor used for providing the centrifugal forces and the bulky fluorescence sensing equipment greatly weakened the portability and the potential for onsite applications. Buffi, et al. [57] applied a different microfluidic device, in which the microfluidic chip contained micro-scale cages with beads to concentrate *E. coli* such that the fluorescence signal was enhanced. The device seemed to offer a smaller configuration and better detection limits compared to the CD-like structure discussed above[59]; however, the portability of the device was not ideal because of the requirements for a microscope[57].

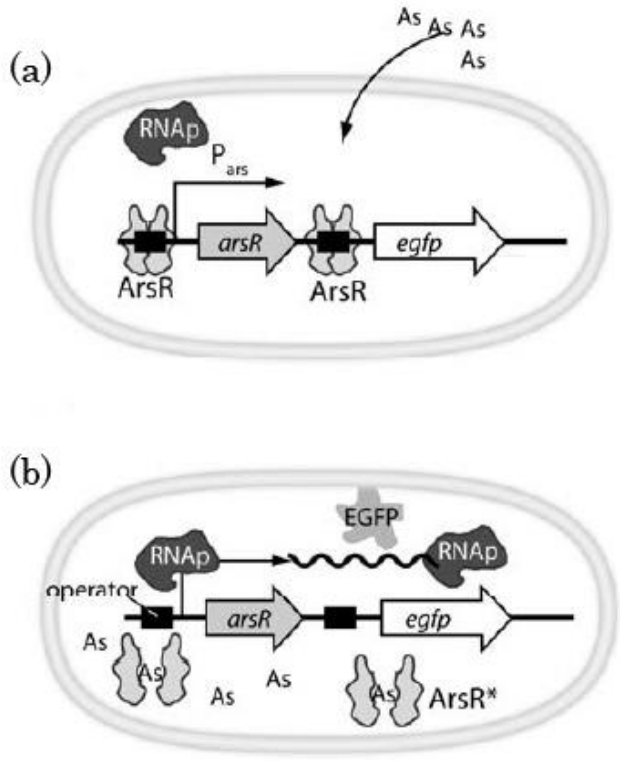

Figure 2.4: Schematics of the biochemical pathway used for arsenite (As^{III}) detection: (a) in the absence of As^{III}, transcription from arsR and the egfp reporter gene is repressed by ArsR; (b) when As^{III} enters the cell, it interacts with the ArsR repressor that undergoes a conformational change (ArsR*) and thus dissociates from its operator. In this way the ArsR gene and the reporter gene are de-repressed, EGFP (*E. coli* green fluorescence proteins) is then produced and fluorescence can be detected.
(Source: Buffi, et al. [57])

A more sophisticated microfluidic device integrated with such whole-cell-based sensors for sensitive As^{III} detection was described by Prindle, et al. [60] (Figure 2.5). In the system, the *E. coli* species was engineered to couple two pathways, the previously discussed As^{III} reporter genes and intracolony

synchronization, to create oscillation signal patterns for detection. The intracolony synchoronization, assisted by the use of H_2O_2, was the key to generate oscillatory signals, and the change of oscillation periods controlled by periodic exchange of H_2O_2 corresponded to As^{III} concentrations. A detection limit as low as 18.3 ppb and a detection range of 18.3 ppb – 75 ppb were reported[60]. In addition, peripheral circuits with data-processing capability and micro-scale optical elements were integrated to enable portable detection of As^{III}. Such integrated design without any additional component or equipment outside of a microfluidic device suggests a likely trend for heavy metal detection (and for other chemical species) on a microfluidic platform. However, the obvious drawbacks were likely long testing time and high system complexity, which may contribute to a high cost of the entire system. In addition, such a system is yet to be tested for real environmental samples.

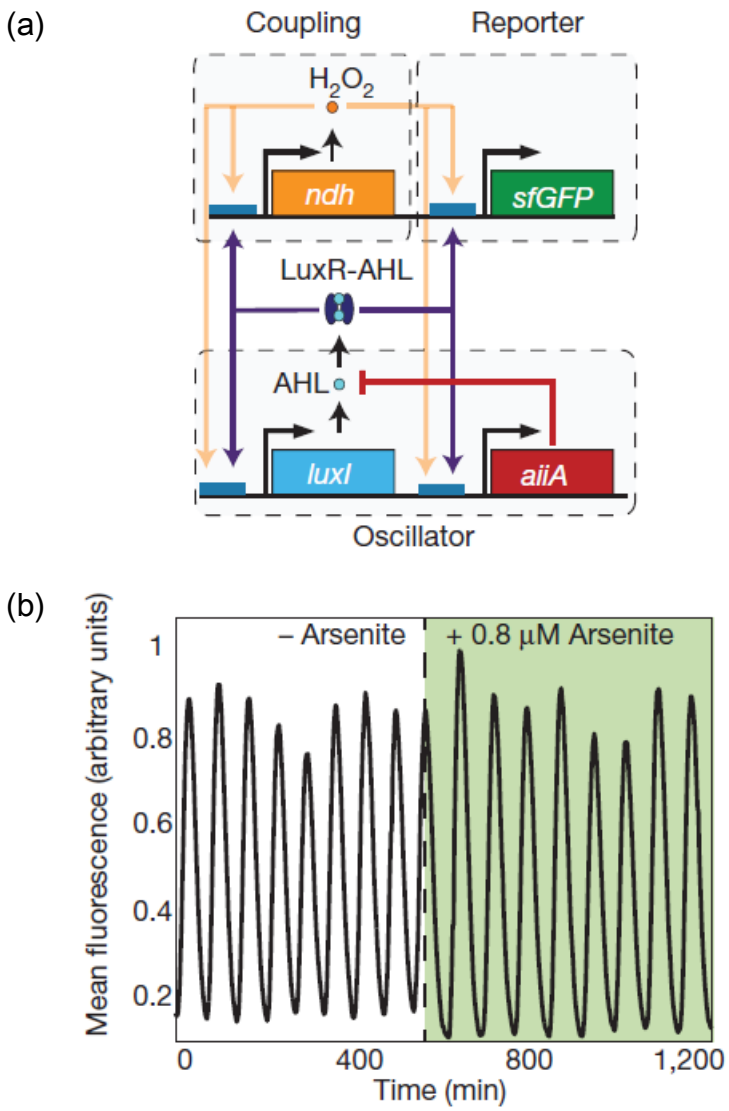

Figure 2.5: The schematic oscillator network and its periodic signal response. (a) Oscillator network: luxI promoter promotes expression of luxI, aiiA, ndh and sfGFP (superfolder variant of GFP) in four identical transcription modules. The quorum-sensing genes luxI and aiiA generate synchronized oscillations within a colony via AHL. The ndh gene codes for NDH-2, an enzyme that generates H_2O_2 vapour, which is an additional activator of the luxI promoter. H_2O_2 is capable of migrating between colonies and synchronizing them. (b) A sample period signal response to an addition of 0.8 µM As^{III}, showing the increment of an oscillatory period from 69 min to 79 min.

(Source: Prindle, et al. [60])

Current studies suggest that short shelf-lives and stringent requirements for growth and storage of sensing bacteria can greatly limit the use of whole-cell sensors for onsite applications[58]. To solve these problems, Date, et al. [61] has reported a special whole-cell-based sensor using the spores of engineered *Bacillus subtilis* and *megaterium*, though the sensors have not been integrated into a microfluidic device. As bacterial spores are highly resilient under adverse environmental conditions, the requirements for spore preservation are much less stringent, for instance, room temperature preservation is likely[58]. In addition, Diesel, et al. [62] suggested that future improvement of whole-cell sensors may be achieved by embedding and drying techniques for in-field assays.

2.3.2 Chemo-sensors

Types of chemo-sensors for heavy metal detection are highly diverse as summarized in Table 2.4. The general approach is to first develop stand-alone assays using existing or newly synthesized chemicals[64], and then introduced them into microfluidic devices[30b, 65]. Fluorescent chemo-sensors refer to those that combine chelators for metal ion recognition with fluorophores to provide fluorescent signals[64g, 65b]. Some chelators themselves can give off fluorescent signals, the intensity of which can be affected by concentrations of target metal ions[65a]. Some chemo-sensors are based on the chemiluminescence

phenomenon (CL), which is the emission of an optical signal during a chemical reaction[64f]. Simple colorimetric chemo-sensors, which show colour responses to the presence of heavy metal ions, are also used in some studies[30b, 30c, 66]. In addition, coupling colorless chelators with GNPs is another interesting way to transform the recognition signal of heavy metals into detectable colour changes from the GNP probes[67].

Table 2.4: Performance and characteristics of microfluidic systems with chemosensors for heavy metal detection

Target	LOD	Detection Range	Advantages	Limitations	Comment	Method	Ref.
Cd^{II} Pb^{II} Hg^{II}	50 µM Unknown Unknown	Not mentioned	Multi-analyte	Insufficient detection sensitivity	Different chemosensors	Fluorimetric chemosensor	*65a*
Hg^{II}	2 ppb	Not mentioned	Low LOD; highly integrated	Complex procedure for synthesis of the sensor		Fluorimetric chemosensor	*64g*
Pb^{II}	5 ppb	< 2.1 ppm (< 10 µM)	Highly integrated, low detection limit	Not portable	Applied for artificial samples	Calixarene-based	*65b*
As^{V}	6.7 ppb (89 nM)	7.5 ppb – 3.8 ppm (0.1 µM – 50 µM)	Low detection limit	Long and complex procedure	Applied to real water samples	Chemoluminescence Spectrometric	*64f*
Cr^{VI}	30 ppb	Up to 5 ppm	Also available for nitrite	Not very portable	Centrifugal system	1,5-Diphenylcarbazide	*66*
Cr^{VI}	50 ppb	0.1 – 20 ppm	Portable and fully-integrated	Unsatisfactory sensitivity	Computer interface, spiked authentic sample tested	1,5-Diphenylcarbazide	*30c*
Hg^{II}	100 ppb (0.5 µM)	200 ppb – 50 ppm (1 – 250 mM)	Fast reaction time	Pumping required	River water samples tested	Colorimetric	*30b*
Pb^{II}	2.1 ppm (10 µM)	0.1 µM	Simple	Peripheral equipment required	Modified GNP	Colorimetric	*67*
Cd^{II}	0.45 ppb	112 ppb (1 µM)	High sensitivity	Interference from Pb^{II}, not portable; SPE required for removing interference		Fluorimetric Rhod-5N	*68*

Fluorescent chemo-sensors on a microfluidic platform have been demonstrated by some research groups. A molecule containing a thiophosphane group as a chelator and a polyoxyethylene group (to improve the solubility of the molecule in organic solvents) was synthesized for the detection of Hg^{II} in an organoaqueous solvent, and an LOD of 2 ppb (10 nM) for Hg^{II} was achieved[64g]. Similar strategies have been used to create fluorescent chemo-sensors that gave LODs of 5 ppb for Pb^{II} [65b] and 0.45 ppb for Cd^{II} [68]. Similar designs were shown for these devices, which included light emitting diodes (LED) as light sources, optical fibers for light transmittance, and photomultiplier tubes (PMT) for signal acquisition. This design had some onsite application potentials, because it provided consistent light conditions regardless of whatever ambient lighting conditions would be in the field. However, the device required peripheral instruments such as a frequency generator, an amplifier and syringe pumps, which greatly limited the portability. Kou, et al. [65a] described a simple microfluidic device for the detection of three heavy metal species (Cd^{II}, Pb^{II}, and Hg^{II}) by using various fluorescent chemo-sensors specific to these ions, though the detection limits (Table 2.4) were yet to be further improved.

Several colorimetric and CL chemo-sensors were also developed for heavy metal ion detection. Nuriman, et al. [30b] developed a novel chemo-sensor, based on a tripodal chromoionophore-PVC film, for selective binding of Hg^{II}, and

demonstrated the use of the sensor in a microfluidic device with a similar configuration as discussed previously[65b]. Som-aum, et al. [64f] described a device that integrated a PMT detector for CL detection of As^{V}. A low LOD (6.7 ppb) was achieved through pre-concentration of As^{V} via sorption to polystyrene beads, as well as the signals given off during the sorption process through chemiluminescence reactions. A masking reagent, ethylenediaminetetraacetic acid (EDTA), was used to eliminate potential interference from co-existing metal cations. Anions such as chromate and phosphate were removed by pre-treatment with anion exchange resins. Selectivity and accuracy for environmental samples were established using several types of water, including drinking water, river water, mineral water, tap water and synthetic lab water. This approach was the only one among all studies reviewed herein that was capable of differentiating As^{V} in the presence of interfering As^{III}. Fan, et al. [67] described a microfluidic platform for Pb^{II} detection, realized by 11-mercaptoundecanoic acid (MUA) modified GNP probes. In the study, Pb^{II} worked as an inducer that triggered the aggregation of the modified GNPs, resulting in a colour change of the GNP probes. The colour changes as detection signals could be spotted by the naked eye, yet the sensitivity (LOD ~ 2.1 ppm) was not satisfactory.

The same chemo-sensors (or other types of sensors) can be applied onto various microfluidic platforms to provide different performances and traits. For

instance, a well-established chemo-sensor for Cr^{VI} was incorporated onto two completely distinct microfluidic platforms[30c, 66]. Comparable detection limits and linear detection ranges have been reported; however, Fralish's[66] method provided better sensitivity (lower LOD), while Segundo's[30c] method was featured with continuous flow desired for long-term monitoring. Other synthetic chemo-sensors that have not been integrated into microfluidic platforms can be found in the review by Aragay, et al. [1]

2.3.3 Electrochemical-sensor

Working principles of electrochemical-sensors are based on potentiometry, amperometry, or voltammetry[69]. Electrochemical-based sensing is one of the most popular methods for portable devices due to the ease of use. The major applications of electrochemical measurement for environmental monitoring are measurements of pH, dissolved oxygen (DO), oxidation-reduction potential (ORP), and various cations and anions. Main advantages of the electrochemical-sensors are reliability, availability of micro-scale probes, multi-analyte capability, suitability for onsite applications, and continuous monitoring[38b, 70]. Several papers have been published to demonstrate the latest microelectrodes for heavy metal monitoring, largely based on stripping analysis or anodic stripping voltammetry (ASV)[71]. Studies have demonstrated that electrodes can be integrated into a

microfluidic platform by screen printing on paper[72], and sample preparation can also be coupled[73]. Compared to the types of sensors described previously, electrodes/microelectrodes can be integrated into microfluidic devices with ease for onsite monitoring.

As the major component of electrochemical-sensors, an electrode can be fabricated out of several types of metals. A mercury electrode is usually used for heavy metal detection based on ASV[74], yet the major concern is potential release of mercury into the environment. Bismuth electrodes have been developed as an attractive alternative to mercury electrodes for ASV analysis of heavy metal ions due to its non-toxic nature and satisfactory performance[75]. For example, Hočevar, et al. [76] fabricated a bismuth-powder modified carbon paste electrode (Bi-CPE), and low LODs of 0.9 and 1.2 ppb for Pb^{II} and Cd^{II}, respectively, have been demonstrated. Jothimuthu, et al. [77] made further advances by integrating a bismuth electrode into a portable microfluidic platform. The working potential window was extended down to -1.9 V, and multiple analytes (Mn^{II}, Zn^{II}, Cd^{II} and Pb^{II}) could be determined simultaneously[77]. Drawbacks of bismuth electrode-based sensors have been reported to be the undesirable memory effect after the stripping step in voltammetry and the short life-time of integrated Ag/AgCl reference electrodes[78]. The performance and characteristics of selected

microfluidic systems with electrochemical-sensors for heavy metal detection are summarized in Table 2.5.

Table 2.5: Performance and characteristics of microfluidic systems with electrochemical-sensors for heavy metal detection

Target	LOD	Detection Range	Advantages	Limitations	Comment	Ref.
Pb^{II} Cd^{II}	0.34 ppm 0.15 ppm	Not provided	Disposable and portable platform	Low sensitivity	Sea water sample tested	72a
Pb^{II} Cd^{II}	2.0 ppb 2.3 ppb	1.0 – 100 ppb	High sensitivity		Paper-based	72b
Pb^{II}	1.0 ppb	Not mentioned	Simple, low cost and portable	No selectivity data	Paper-based	79
Mn^{II} Zn^{II} Cd^{II} Pb^{II}	Not mentioned	Not mentioned	Working potential window down to -1.9 V	Not pragmatically tested	Bi as working electrode; Ag/AgCl as reference electrode	77
Pb^{II}	0.55 ppb	1 – 1000 ppb	Highly reusable, low LOD	Selectivity information limited		78

Other types of electrodes such as Ag[78], Ag/AgCl[72a] and carbon electrodes[72b, 79] have been demonstrated for heavy metal ion detection using microfluidics. Jung, et al. [78] adopted an electrochemical sensor, which consisted of a silver electrode as the working electrode and an integrated silver counter and quasi-reference electrode for Pb^{II} detection with a wide detection range (1 –

1000 ppb). This sensor was integrated into a compact system composed of a microfluidic chip and a portable potentiostat with a laptop interface for measurements and data analysis, which made the whole system portable for potential onsite applications. It was verified that the reusability of such an electrode was greatly improved over a bismuth electrode and a relative standard deviation (RSD) was shown to be only 1.0% from forty-three consecutive measurements. Zhou, et al. [72a] developed a microfluidic device that required a very small sample volume by using a nanometer-size channel connected to a reservoir. An Ag/AgCl reference microelectrode was used in the microfluidic chip for the detection of Pb^{II} and Cd^{II} and LODs of 0.34 and 0.15 ppm, respectively, were demonstrated. A recent study for detection of the same metal ions with carbon electrodes on a disposable and low-cost paper-based device has been shown by Shi, et al. [72b] (Figure 2.6), and the LOD was reported in the ppb levels for both analytes. A water sample could be introduced to the device detection zone through the capillary force of another paper strip without the use of a pipet or a dropper. The device has been tested using real environmental samples (salty soda water and groundwater) and good tolerance to interferences was demonstrated. Nie, et al. [79] also fabricated a paper-based device with the use of an electrochemical sensor for the detection of Pb^{II}. A LOD of 1 ppb has been claimed, but no selectivity data were provided.

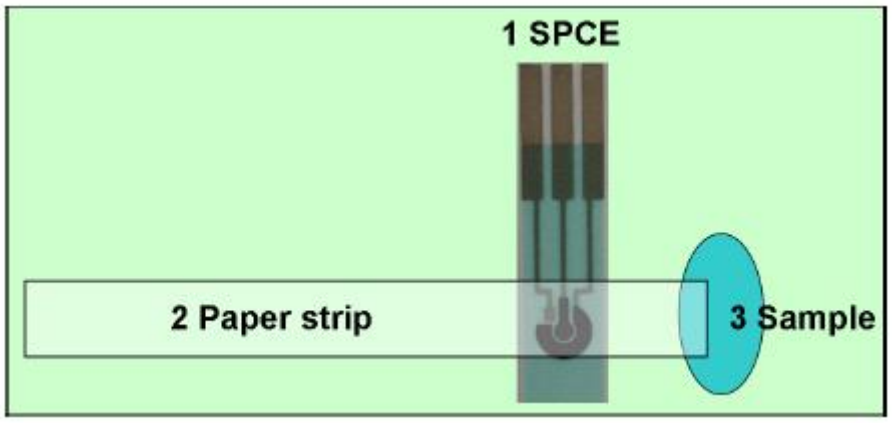

Figure 2.6: Schematic layout of a paper-based electrochemical sensing device. The sensor comprises (1) a screen-printed capillary electrode (SPCE), (2) a paper strip and (3) a sample cell.
(Source: Shi, et al. [72b])

2.4 Discussion and Future Trends

We compared the performance of all types of sensors discussed above for a certain heavy metal analyte, and those with the best performance are summarized in Table 2.6. Electrochemical sensors are the only type that is absent because of its low sensitivity in general. Surprisingly, many of the devices provide even better sensitivity than traditional analytical instruments, such as those for Pb^{II}, Hg^{II}, Cd^{II} and Cr^{VI} detection. The paper-based device presented by Zhang, et al. [48] can detect Pb^{II} at even ppt levels based on a nucleotide-based sensor combined with nano-materials.

Table 2.6: Summary of the sensors reviewed herein providing the highest sensitivity for different types of heavy metal analytes.

Target	Sensor Type	LOD	Detection Range	Signal acquisition method	Ref.
Pb^{II}	Nucleotide-based biosensor	2.1 ppt	6.2 ppt – 207 ppb (30 pM – 1 μM)	ECL	*48*
Hg^{II}	Nucleotide-based biosensor	40 ppt	0.1 – 200 ppb (500 pM – 1 μM)	ECL	*48*
Cd^{II}	Chemosensor	0.45 ppb	Up to 112 ppb (Up to 1 μM)	Fluorescence	*68*
Cr^{VI}	Protein-based biosensor	40 ppt	0.03 – 1 ppb	Fluorescence	*33*
As^{III}	Whole-cell-based biosensor	7.5 ppb	Up to 0.1 mM (Up to 7.5 ppm)	CL	*61*
As^{V}	Chemosensor	6.7 ppb	7.5 ppb – 3.8 ppm (0.1 μM – 50 μM)	CL	*64f*
Zn^{II}	Whole-cell-based biosensor	7.5 ppb	65 ppb – 6.5 ppm (1 μM – 100 μM)	Fluorescence	*61*

Despite the advances made in the past decade, current microfluidic devices are yet to be made highly portable, reliable, sensitive and capable for onsite analysis for heavy metals. The major limitations are the inability to analyze metal speciation and the lack of demonstrated success in real environmental water samples, among others. None of the devices discussed were able to provide speciation information, which is critical for environmental monitoring because the same heavy metal ions with different oxidation status might exhibit

distinct toxicity and mobility[80]. Only one approach illustrated the feasibility for the detection of As^{V} [64f] in the presence of both As^{V} and As^{III}. In the meantime, only a number of studies challenged their devices by real water samples[30, 48, 56, 64f, 72a], while most only tested standard solutions in a clean matrix or artificial samples prepared in laboratories. However, the real challenges come from complex compositions of real environmental samples (e.g. sea water, surface water, tap water) that may be high in alkalinity, salinity, turbidity or other metal ions that could cause significant interferences.

One future trend involving microfluidic devices for heavy metal detection is the integration of nano-materials to improve the sensitivity. Devices will be made either simple for rapid and economic testing, or fully integrated to be robust enough, potentially to replace traditional analytical instruments or for monitoring water quality remotely and autonomously. In addition, there are other approaches to improve selectivity and sensitivity, such as the use of a masking agent to hide interfering ions[47], or improving electrode materials[77].

2.4.1 Integration of nano-materials

The use of nano-materials to enhance selectivity, sensitivity, and reproducibility plays a crucial role in the future development of a sensitive heavy metal sensing device[1]. Nano-material-based sensors, such as inorganic quantum dots (QDs)[81],

plasmonic sensors[15-16, 82], and composite sensors (e.g. QD – DNA – GNP)[44] exhibit excellent performance for heavy metal ion sensing. As the detection in those sensors is optical based, they are of high compatibility with optical microfluidic devices that share similar designs. Integration of novel nano-materials into a 3D paper-based microfluidic device (Figure 2.7) has been realized by Zhang, et al. [48] to achieve excellent performance.

In this device, fluorescent carbon nanocrystals (CNCs) were used to provide ECL signals while silica nanoparticles were employed for immobilization of CNCs onto the paper-based device to yield a high loading and thus to enhance signal intensity and sensitivity. Besides, the Ruthenium-GNPs (Ru@GNPs) used for the detection of Pb^{II} in parallel could be easily incorporated into a nucleotide-based sensor while exhibiting ECL behaviour[48]. The combination of the nucleotide-based biosensor with the nano-material provided sensitive recognition of the target metal ions as well as high signal intensity. LODs of 2.1 and 40 ppt for detection of Pb^{II} and Hg^{II}, respectively, were achieved, which are considerably lower than the ppb level of LODs provided by conventional analytical methods (e.g. ICP-AES[4]).

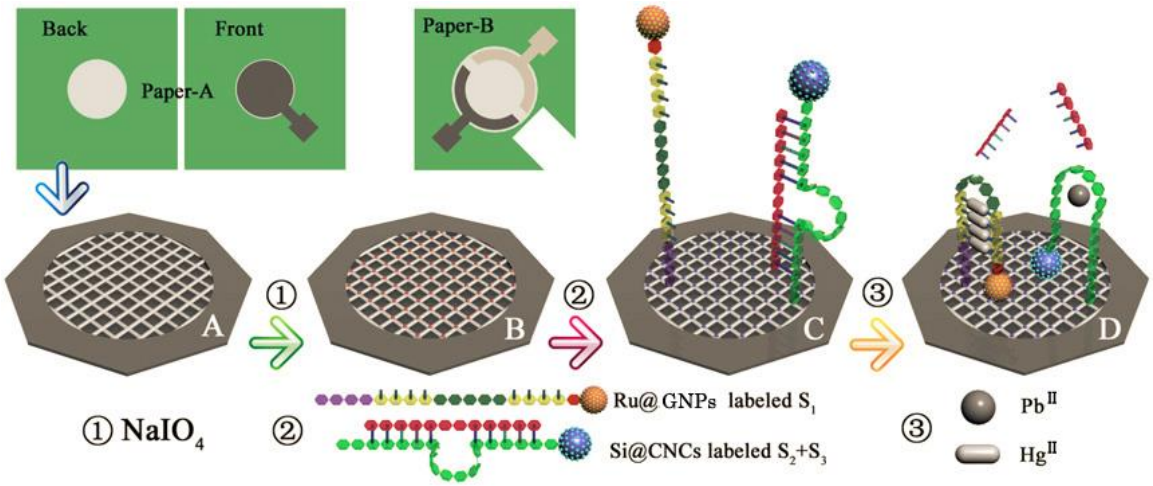

Figure 2.7: Schematic structure of a 3D paper-based ECL device and the reaction zone of the immunoassay on the back of wax-patterned paper. ① The paper was treated by $NaIO_4$; ② after immobilization of the ECL reporters (Ru@GNPs labeled DNA strands for Hg^{II} and Si@CNCs labeled DNA strands for Pb^{II}); and ③ detection of the targets: capturing Pb^{II} and Hg^{II}.
(Source: Zhang, et al. [48] with minor modifications)

2.4.2 Application of paper-based device

The development of paper-based microfluidic devices is a major breakthrough compared to conventional microfluidic devices for three main reasons: extremely low cost (~6 m^2 of high-quality chromatography paper can be made into thousands of paper devices)[83]; ease of fabrication (patterning by simple cutting and wax printing)[83-84]; and compatible to many bio/chemical assays[83], including electrochemical[45, 85], colorimetric[86], immunoassay[87], and enzyme-based[88] assays. Many researchers have taken advantage of the high compatibility of paper-based devices for environmental monitoring, especially for water quality monitoring[48, 55, 72b, 79]. Successful integration of an electrochemical sensor onto a paper-based

device is shown in Figure 2.8. In this device, layers of different types of paper were stacked vertically to create a microfluidic channel used for sample loading, and to define the detection zone where electrodes were located[79]. Anodic stripping analysis was performed for the detection of Pb^{II} and a low LOD was achieved on this device (Table 2.6), indicating the good compatibility of paper-based devices with electrochemical sensors.

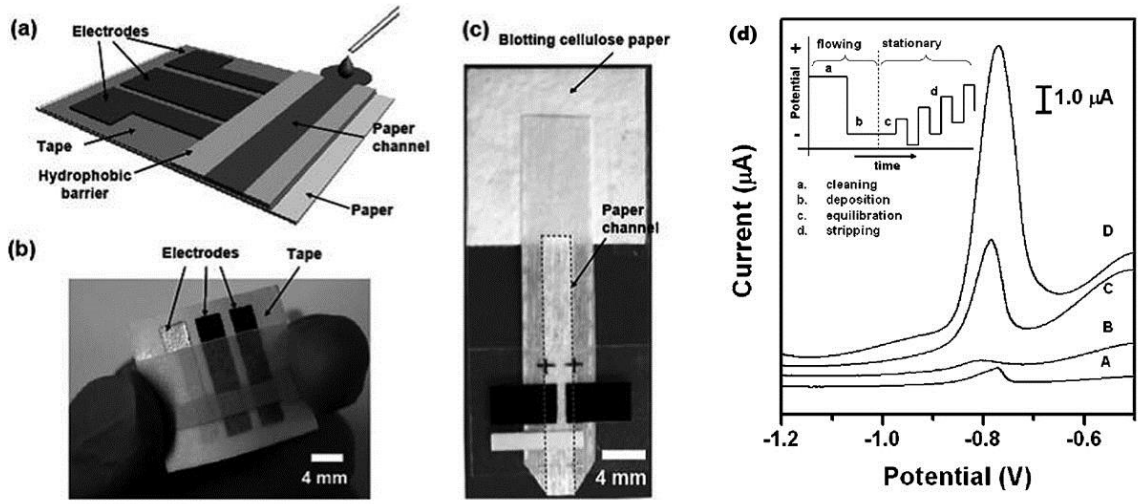

Figure 2.8: (a) Schematics of a paper-based device coupled with an electrochemical-sensor with the structures in detail (b), and a hydrodynamic paper-based electrochemical sensing device for the measurement of heavy metal ions. (c) The device consists of two printed carbon electrodes as the working and counter electrodes, and a printed Ag/AgCl electrode as the pseudo-reference electrode. (d) Results of ASV analysis of Pb^{II} by this device.
(Source: Nie, et al. [79])

Besides the aforementioned advantages, there are many other important features of paper-based devices that lead the future trend of simple and accessible microfluidic platforms. One important feature is that operation of paper-based devices does not require external energy for solution transportation or mixing[83]. In addition, several paper layers can be stacked in a certain format to perform assays in 3-dimensional patterns[83, 87b, 89], which enables paper-based devices to be used for more complex assays, such as detection of multiple analytes in parallel. Moreover, coupling a paper-based device with a commercialized reader (e.g. personal glucose meters) provided another approach for rapid and low-cost detection[88b], because the glucose meters are readily available and easy to operate. Yet the one major obstacle of coupling such glucose meters has been the limited number of detectable targets (usually glucose only)[90]. Xiang and Lu [88b] made a breakthrough in this field as they demonstrated the feasibility of using the glucose meter for measurement of other analytes including the toxic metal ion uranium (Figure 2.9). As illustrated in the figure, when the special DNA sequence recognized a target analyte, the enzyme (invertase) conjugated onto the DNA would be released, and then catalyze hydrolysis of sucrose to form glucose. As the analyte concentration is proportional to the amount of glucose produced, the measurement of glucose by the meter can be used for quantification of the analyte of interest. In the future,

by developing more metal-specific nucleotide-based sensors, the use of glucose meters can be expanded for analyses of other heavy metal ions in solution, with high portability, sensitivity and selectivity.

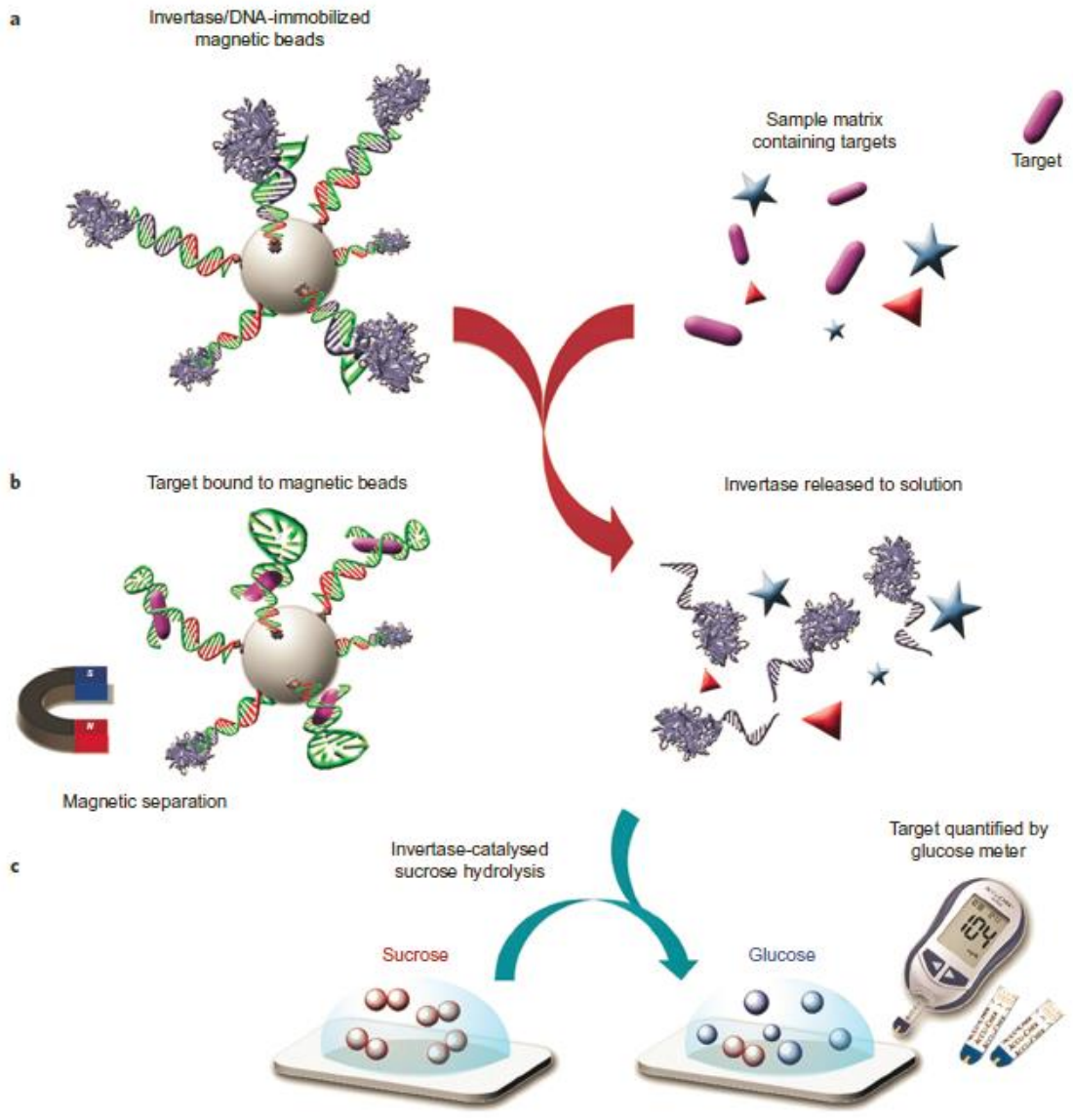

Figure 2.9: Schematics of a method using a personal glucose meter to detect several analytes beyond glucose.

(Source: Xiang and Lu [88b])

2.4.3 Micro-Total Analysis Systems

A fully integrated system, or so-called micro-total analysis systems (μTASs), is considered to be the ultimate goal for environmental analysis, as well as for other types of analysis such as in medical fields. Such a device may contain several elements to separate and concentrate a target of interest (especially for heavy metal ions in trace levels) so as to achieve high sensitivity. Integration of sample preparation techniques such as solid-phase extraction (SPE)[56] and capillary electrophoresis (CE)[46] can not only improve the sensitivity for trace heavy metal detection but also minimize the impact of interference, as the target is separated from the bulk solution and/or concentrated.

A trend of designing μTASs is to combine a microfluidic device with telecommunication technologies to enable the use of such devices in remote areas, and the major benefit, among others, is allowing μTASs to be more accessible to non-experts for sophisticated analysis. Martinez and his coworkers[89c] demonstrated the idea of using a mobile phone for imaging of the colorimetric results from their paper-based microfluidic device and for transmitting the data wirelessly to the lab where the analysis would be performed (Figure 2.10). Another advanced microfluidic device demonstrated by Chin, et al. [91] combined cell-phone and satellite communication technologies for performing

enzyme-linked immunosorbent assays (ELISA), allowing analysis or monitoring in resource-limited areas with laboratory-level accuracy[91] (Figure 2.11).

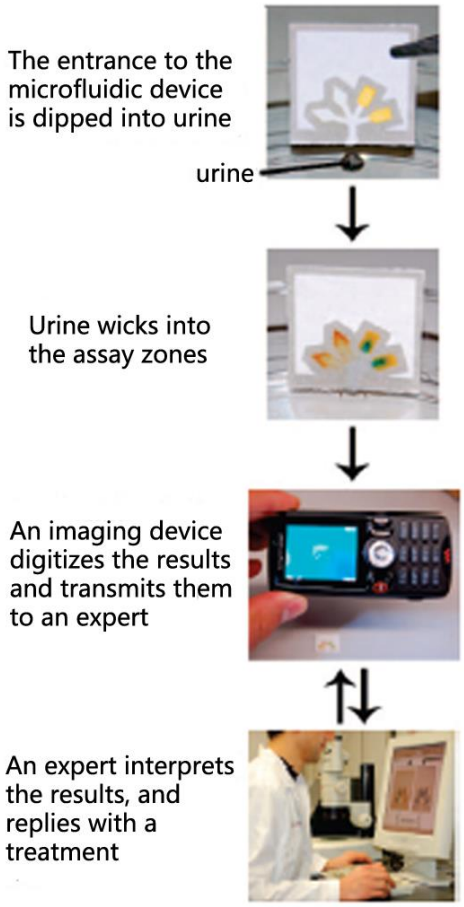

Figure 2.10: A general strategy for low-cost remote diagnosis or measurements and precise offsite analysis by experts
(Source: Martinez, et al. [89c] with minor modifications)

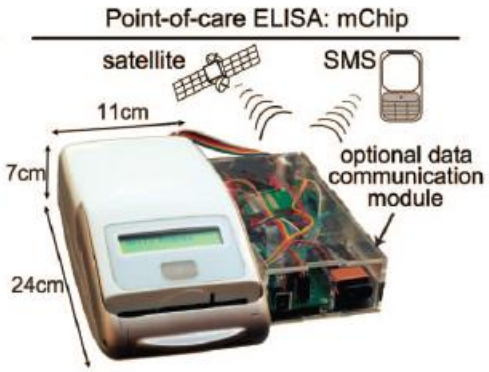

Figure 2.11: Overview of a microfluidic chip device with a wireless module for onsite ELISA
(Source: Chin, et al. [91])

2.5 Conclusions

Great efforts have been made to develop microfluidic devices for rapid, cost effective and sensitive detection of aqueous heavy metal ions. Many different types of bio-, chemo- and electrochemical-sensors have been designed and demonstrated, and high sensitivity has been achieved in some cases. However, most of the work did not test the devices with real environmental samples and challenges from matrix interference still remain. As a matter of fact, many devices show greatly reduced sensitivity or even experience total failure when real water samples are applied. Future work to address these problems and to provide better performance as well as lowering the cost for determination of trace heavy metal content is as such: (i) to introduce nano-materials for better sensitivity, (ii) to develop paper-based devices to improve portability and lower

the cost, (iii) to integrate more components for sample preparation and remote communication to achieve better performance and easy operation.

CONNECTING PARAGRAPH

It is clearly pointed out in Chapter 2 that the use of nano-materials is one of the future trends for detection of heavy metals with high sensitivity and selectivity. GNP probes have common optical signal patterns, which are highly desired for microfluidic devices, so that an optical reader can be used to detect various targets. In addition, label-free GNP probes (described in Chapter 1) share great advantages for rapid and simple tests, such that they have considerable potential for onsite applications. Therefore, a new assay based on label-free GNPs as probes was developed for lead detection in aqueous solutions, as demonstrated in the next chapter. For target recognition, GSH was chosen as the bio-sensor because of its low cost compared to other customized peptides[5, 20].

CHAPTER III A RAPID AND SENSITIVE COLORIMETRIC ASSAY FOR LEAD DETECTION BASED ON LABEL-FREE GOLD NANOPARTICLES (GNP) AND GLUTATHIONE (GSH)

(A draft prepared for submission to *Analyst* as a communication paper)

3.1 Abstract

A rapid and sensitive colorimetric method for lead (Pb^{II}) detection has been developed by utilizing the unique optical properties and surface chemistry of gold nanoparticles (GNPs). GNPs are used as a label-free colorimetric reporter and glutathione (GSH) as a linker. The presence of Pb^{II} greatly promotes aggregation of the GNPs, and the level of aggregation can be quantified by UV-Vis spectrometry, leading to an accurate determination of Pb^{II} concentration in aqueous solutions. No modification of GNPs prior to the application is required thus eliminating strict reagent preservation requirements. The limit of detection (LOD) of 6.0 ppb achieved by the method is lower than the maximum acceptable lead concentrations (10 - 15 ppb) in drinking water, indicating its high sensitivity and potential applicability in drinking water testing. The high selectivity for Pb^{II} against ten metal ions has been demonstrated, and several masking agents were

evaluated for their effectiveness in reducing potential inferences from an additional four metals.

3.2 Introduction

Lead is known for being highly toxic, carcinogenic and bioaccumulative[92]. It can cause renal malfunction and inhibit brain development, especially in children[17a, 93] and pose a high risk to human health even at trace levels. One of the well-recognized major exposure routes to human is through the drinking water provided by municipal water treatment plants[94]. The WHO, the Health Canada and the U.S. EPA have issued guidelines on lead in drinking water, setting the upper permissible limit at 10 ppb, 10 ppb and 15 ppb, respectively[3, 63, 95]. These limits demand high performance on analytical methods for lead detection, such that only those which have sufficient sensitivity can be applied. Analytical techniques such as atomic absorption spectrometry (AAS) and inductively-coupled plasma atomic emission spectrometry (ICP-AES) are frequently used since they provide limits of detection (LOD) as low as 1 ppb for lead[4]. However, these techniques require highly sophisticated and costly equipment and consumables[5]. They are also limited by their bulkiness, the need for highly skilled analysts and non-suitability for onsite applications[6]. Therefore, there is a great demand for low-cost, simple detection methods with sufficient sensitivity to be

developed, which can supplement or replace conventional methods. A recent event that highlights the need for rapid and low-cost lead detection method is the incidence of elevated lead levels in Washington D.C. drinking water, where about a million people had been exposed to lead levels higher than the limit of US drinking water guidelines for almost 4 years[96].

GNPs, as crucial and frequently used materials in nanotechnology[97], have been widely applied in many fields, such as cancer diagnosis[98], drug delivery[99], bio-sensing[8], and environmental monitoring[16, 47, 100]. The wide use of GNPs is mainly attributed to their unique surface chemistry and optical properties. Several researchers have developed assays to utilize GNPs for environmental monitoring of heavy metal ions in water and LODs down to around 10 ppb have been reported. Nucleotide-based sensors coupled with GNPs have been shown to be sensitive and selective[9, 82a, 101]; however, strict preservation conditions (such as very low temperature) of these sensors greatly limited the use of the assays for onsite applications. Chai, et al. [17a] and Mao, et al. [102] employed glutathione (GSH)-modified GNPs, but still faced a similar challenge of preserving modified GNPs without rapid loss of intended functions.

In this study, we have demonstrated that label-free GNPs can be used for heavy metal detection (lead as an example) in a simple and rapid assay, yet with sufficient sensitivity and selectivity. GNPs and other reagents can be stored at

room temperature with reasonable shelf lives. During the assay, the thiol-containing ligand (GSH), which has been reported to have a high affinity for Pb^{II} [103] and has been used for its detection[17a, 102], is used to conjugate the non-modified GNPs through its thiol group. The presence of Pb^{II} will promote aggregation of spherical GNPs to result in a decrease in the plasmonic absorption at around 520 nm and the formation of a peak at a longer wavelength band[10]. The corresponding significant colour changes can be detected by the naked eye, and measured by UV-Vis spectrometry to allow for quantification. The selectivity of the assay towards Pb^{II} as opposed to other heavy metal ions has also been evaluated, and measures to reduce potential interferences have been tested.

3.3 Experimental section

3.3.1 Reagents and materials

Gold (III) chloride trihydrate ($HAuCl_4$, 99.9%), Ethylenediamine tetraacetic acid disodium salt (EDTA, ≥99.0%) and GSH (L-Glutathione reduced, ≥98.0%) were obtained from Sigma-Aldrich. Potassium phosphate monobasic (ACS), dibasic anhydrous (ACS), sodium citrate dihydrate (≥99), sodium fluoride (NaF, ACS), 5-sulfocylisilic acidand sodium chloride (NaCl, ACS) were obtained from Fisher Scientific. Deionized water was purchased from Thermo Scientific.

3.3.2 Synthesis and characterization of GNPs

All glassware used in the following procedures were bathed in an acid solution (1N of HCL) for more than 48 h, followed by thorough water rinsing and drying in air prior to use. The GNPs were synthesized using the classic Turkevich – Frens method[34] and the protocol developed by Liu and Lu [35] was followed with a few minor modifications. A solution of $HAuCl_4$ (100 mL, 1 mM) was heated to boiling in a flask with a condenser. Then a sodium citrate solution (10 mL, 38.8 mM) was added, and the boiling was continued for an additional 30 min after the solution turned from pale yellow into ruby red. The final GNP aqueous solution was stored at 4 °C prior to the assay.

GNPs were imaged via transmission electron microscopy (TEM) using a Tecnai GF20 system operated at 200 keV. The sample was prepared by dipping a copper grid coated with an ultrathin layer of carbon into a GNP aqueous suspension, followed by drying in ambient air for 5 min. The size distributions of the GNPs were determined using ImageJ.

3.3.3 Spectrometric detection of Pb^{II}

The detection of Pb^{II} in water was realized by monitoring the aggregation behaviour of the GNPs in the presence of GSH, and changes in absorbance of the assay solutions were measured using UV-Vis spectrometry. The assay was

performed in clear-bottom 96-well plates (Costar®). The GSH solution was freshly prepared in the presence of a background electrolyte (NaCl) and a potassium phosphate buffer. The assay was started by mixing 150 µl of a water sample with the GSH solution, followed by addition of 100 µl of the GNP aqueous solution (~13 nM)[35]. The final concentrations of NaCl, GSH and the phosphate buffer (pH = 7) in the 300 µL assay solution were 10 mM, 4.1 mM, and 2.6 mM, respectively. After sufficient mixing by pipetting was performed, the assay solution was maintained at room temperature for 2 min. The absorbance of the assay solution was then recorded at wavelengths of 520 nm and 610 nm (SpectraMax M5) every minute, for 15 minutes. A spectrum scan ranging from 480 to 680 nm was also recorded. The time profile of the absorbance ratio at two wavelengths (A_{610}/A_{520}) was reconstructed in Microsoft Excel.

3.4 Results and Discussion

3.4.1 Mechanism of the colorimetric assay for lead

GSH is a tripeptide with a gamma peptide linkage between the amine group of cysteine and the carboxyl group of the glutamate side-chain, and it can be used as a linker to cause aggregation of GNPs. The thiol-group (-SH) has a high affinity towards gold and an Au-S covalent bond is expected to be formed during this process[12]. Simultaneously, GSH molecules form intermolecular hydrogen

bonding among themselves, even when the GSH molecules are adsorbed to the surfaces of GNPs. Therefore, the combination of such molecular interactions enables GSH to aggregate GNPs under certain conditions[104]. However, it has been found that GSH-mediated aggregation of GNPs progresses very slowly, probably because of the weak hydrogen bonding. Beqa, et al. [17c] has reported that lead (Pb^{II}) can strongly induce aggregation of GSH-modified GNPs at certain pH levels through formation of coordination complexes between Pb^{II} and the carboxyl group ($–COO^-$), two of which are present in each GSH molecule[17c, 103a]. Therefore, the addition of Pb^{II} to an aqueous solution can greatly enhance the rate of GNP aggregation in the presence of GSH, and much faster colour changes can be observed accordingly (Figure 3.1).

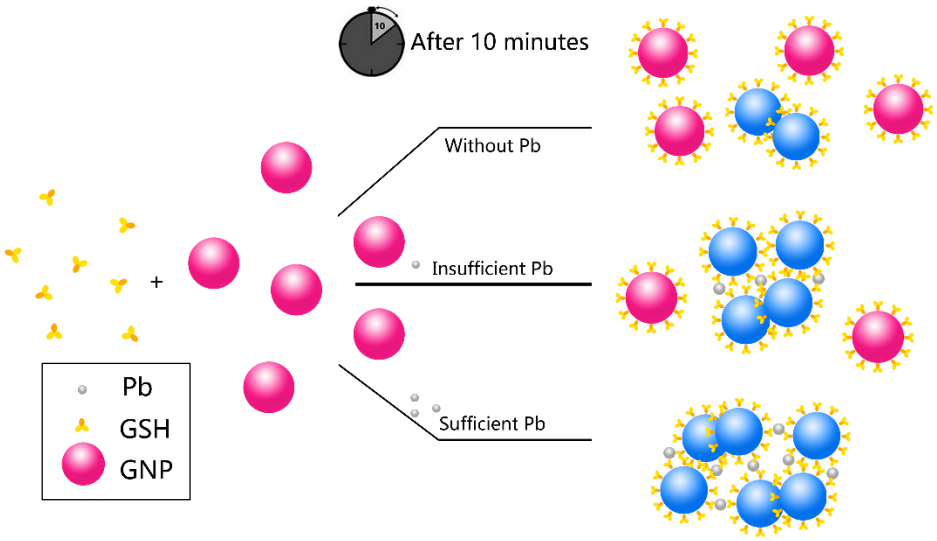

Figure 3.12: Schematics of the time-dependent determination of the Pb^{II} concentration. The aggregation rates vary according to the concentration of Pb^{II}.

3.4.2 Spectrometric detection of Pb^{II}

The average diameter of the GNPs synthesized in the study was determined to be 15.2 ± 3.6 nm based on TEM images (Figure 3.2a), and the narrow size distribution could be important to ensure high sensitivity because of the relatively homogenous optical properties. The GNP aqueous solution had a characteristic absorbance peak at ~520 nm, giving an intense ruby red colour (Figure 3.2b) due to the surface plasmon resonance (SPR) of the GNPs[105].

(a) (b)

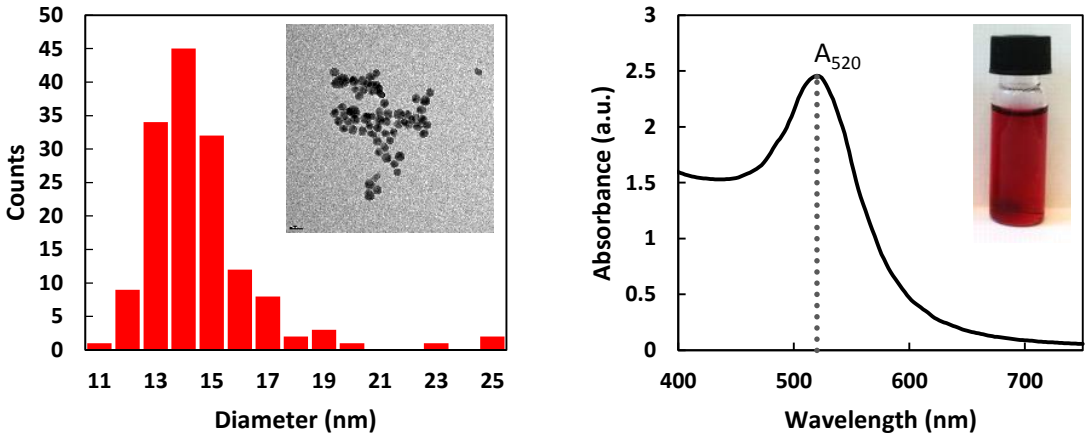

Figure 3.2: Characteristics of the GNP aqueous solution: (a) size distribution and TEM image; and (b) characteristic absorbance peak at 520 nm of the solution, showing ruby red colour.

In the study, we used the relative absorbance ratio at 610 and 520 nm (A_{610}/A_{520}) to describe the aggregation state of GNP solutions, rather than the absolute

absorbance at a single wavelength, which has been used in other studies[17a, 106]. It was observed through spectrum scanning that as GNPs were aggregating (mediated by GSH), there were apparent changes of two absorbance peaks. The absorbance peak at 520 nm was decreasing while the absorbance peak at 610 nm (and at higher wavelengths) was increasing (Figure 3.3a). The red shift and broadening of the peak at 520 nm have been reported due to the collective effect of the SPR[17a] from particles of different sizes. The intensity ratio of the two absorbance peaks was found to be a more sensitive parameter to indicate the aggregation state of the GNPs, and therefore was used throughout the study. An example of time profiles of GNP aggregation promoted by the addition of Pb^{II} using A_{610}/A_{520} versus time is shown in Figure 3.3a with the corresponding colour changes in Figure 3.3b. The absorbance readings and images of the assay solutions were taken at 2, 5, 10 and 15 min. The colour of the GNP solutions gradually changed from violet to purple, and further changed to blue in the presence of Pb^{II}, indicating the promotion of GSH-mediated aggregation by Pb^{II}. Figure 3.3b shows the colour changes of the control (GSH + GNPs) and an assay solution at a concentration of 2 ppm of Pb^{II}, while the time profiles at other concentrations are shown in Figure A1 in the Appendices.

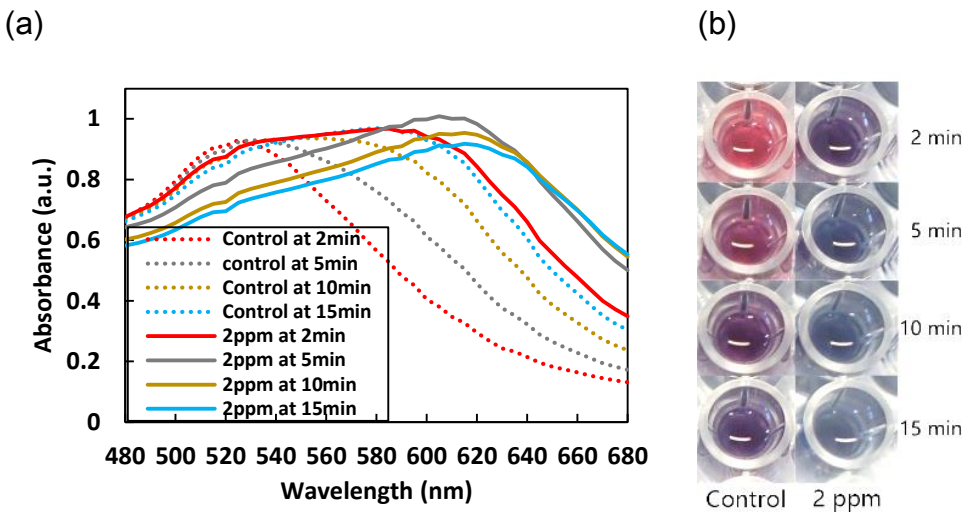

Figure 3.3: (a) The UV-Vis spectrum of evolution of the absorbance peak of the control (dotted lines) and 2 ppm lead standard solution (solid lines) over time, and (b) the colour changes corresponding to different incubation times.

The aggregation kinetics of GNPs in the assay was investigated using standard Pb^{II} solutions in four replicates ranging from 5 – 2,000 ppb (Figure 3.4a). As shown in the figure, the aggregation kinetics was a function of Pb^{II} concentration, and the kinetics reflected by the absorbance ratio of A_{610}/A_{520} was proportional to the level of Pb^{II} added to the assay. At the highest concentration of 2,000 ppb, the aggregation of GNPs quickly reached a plateau in less than 2 min, while at lower concentrations (e.g. 5 - 505 ppb) the aggregation had not reached a plateau by the end of 15 min. As the highest sensitivity (highest value of A_{610}/A_{520}) was achieved when the assay incubation time was around 8 - 11 minutes (when concentrations were no more than 505 ppb), we chose 10 min as the detection time. The calibration curve (four replicates for each data point)

generated at the detection time of 10 min had a linear range of 5 ppb – 505 ppb with R^2 = 0.9929 (Figure 3.4b). The LOD was determined to be 6.0 ppb, which was lower than the upper permissible limit of Pb^{II} in drinking water in Canada[3], indicating its high sensitivity and the potential to be used for daily water quality monitoring.

(a)

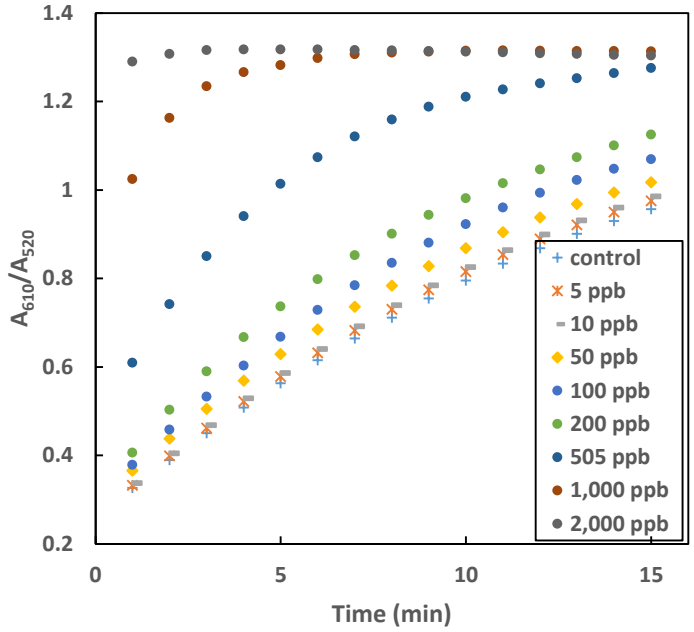

(b)

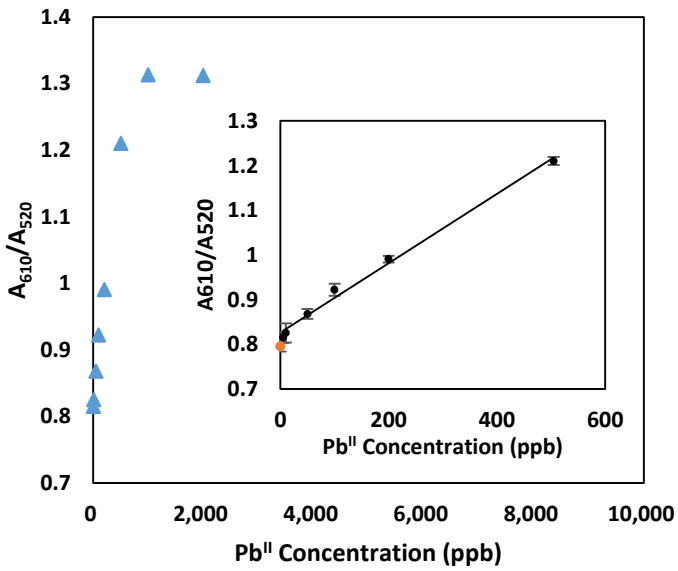

Figure 3.4: (a) Evolution of the ratio (A_{610}/A_{520}) from 5, 10, 50, 100, 200, 505, 1,000, 2,000 ppb over time. (b) Response of different concentrations of lead standard solutions. The inserted chart demonstrates the calibration curve (with R^2 = 0.9929) for the linear range. All the data were measured at 10 min based on 4 independent measurements. The orange dot represents the control without addition of lead.

3.4.3 Selectivity Test

Selectivity of the assay for Pb^{II} detection was evaluated using fourteen metal ions (Ca^{II}, As^{III}, Mg^{II}, Hg^{II}, Cu^{II}, Ni^{II}, Fe^{III}, Ba^{II}, Co^{II}, Ag^{I}, Mn^{II}, Cd^{II}, Zn^{II}, Cr^{III}, Al^{III}). The same assay was conducted, where each metal ion at 1 μM was added instead of Pb^{II}, and the absorbance ratio was also recorded at the detection time of 10 min. The relative signal intensity of the metal ion to that of Pb^{II} at 1 μM was calculated. As shown in Figure 3.5, most of the metal ions had negligible impact on the assay at 1 μM, suggesting high selectivity for Pb^{II} over other metal ions. Among the fourteen metal ions, Cr^{III} was most likely to interfere with the detection of Pb^{II} as it had the highest signal, ~25% of Pb^{II}, at the same molar concentration of 1 μM[107]. Other metal ions exhibited negligible responses, less than 10% of that of Pb^{II} (Figure 3.5), indicating that the assay is highly selective for Pb^{II}.

In a separate test where the fourteen metal ions as well as Pb^{II} were tested at the same mass concentration of 200 ppb rather than the same molar concentration, the interferences from Al^{III}, Zn^{II}, Cd^{II} and Cr^{III} were more evident. The relative signal intensities (to that of Pb^{II}) were 150%, 63.3%, 45.2% and 44% for Al^{III}, Zn^{II}, Cd^{II} and Cr^{III}, respectively. The discrepancy between the two tests (at 1 μM and 200 ppb, respectively) was due to the relatively lower molar mass of these ions compared to Pb^{II} (Figure A2). Fuhr and Rabenstein [108] reported

that Cd^{II} and Zn^{II} showed a high affinity for GSH to form complexes, which agrees with the data shown in Figure A3 (in the Appendices) that these two ions could be potential inferences for the assay. Chen, et al. [109] observed that Al^{III} could destabilize citrate-capped GNPs, which are the types of GNPs used in the study, to result in aggregation. Wang, et al. [110] also found that Al^{III} was able to form a complex with GSH in acidic aqueous solutions in the similar fashion to Pb^{II}. As those ions could be problematic interferences, it was necessary to investigate methods to reduce such interferences to avoid false positive results.

Methods to minimize the impact of those interfering ions have been explored by the use of several masking agents, which were selected based on their high formation constants with the interfering ions. The tests were conducted in a pair-wise fashion with Pb^{II} and one of the interfering metal ions, both at 200 ppb (Al^{III} - 7.7 µM, Cd^{II} - 1.8 µM, Cr^{III} - 4.0 µM), with the addition of a masking agent. The results were shown in Figure A3 in the Appendices. It was clearly shown that EDTA (1 µM) could effectively mask Cr^{III}, attributed to EDTA's higher formation constant with Cr^{III} compared to Pb^{II} [111], and the response in the presence of both Pb^{II} and Cr^{III} was only slightly higher (~10%) than the response from 200 ppb of Pb^{II} alone. A similar result was shown for Al^{III} when masked by EDTA, even though the formation constant of Pb^{II} with EDTA is only slightly higher than that of Al^{III} [111]. Cd^{II} was found to be slightly masked by a mixture of

NaF (5 μM) and 5-sulfosalicylic acid (5 μM)[112], and a reduction of the response by 11.5% is observed. Though the co-presence of these ions with Pb^{II} in water intended for human consumption is not often expected, further tests are still needed to optimize the use of masking agents to reduce the likelihood of false positives for real water samples.

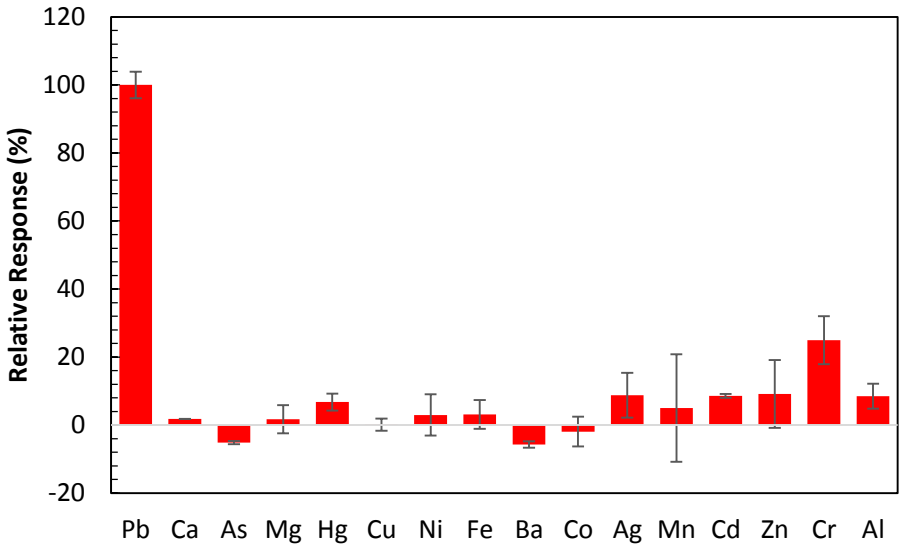

Figure 3.5: Selectivity test of the Pb^{II} sensor with the relative response of each ion with respect to Pb^{II} as 100%. Fourteen interfering ions are tested in the presence of 1.0 μM each and the error bars represent the standard deviation of the samples.

3.5 Conclusions

In this study, a rapid and simple label-free assay using GNPs for sensitive Pb^{II} detection in water has been demonstrated without the use of corrosive or

hazardous agents. Compared to other assays using GNPs for metal ion detection in the literature, our approach is much simplified by eliminating the need to modify GNPs, and therefore has a greater potential for field applications. The LOD of this assay conducted using DI water spiked with Pb^{II} was 6.0 ppb, lower than the WHO limit for drinking water of 10 ppb. The current assay with a detection time of 10 min has a linear dynamic range from the LOD up to ~500 ppb. The detection can be easily realized using a spectrometer. A future study to minimize the impact of interfering ions could bring the assay much closer to real world applications.

CONNECTING PARAGRAPH

The method developed in Chapter 3 is rapid and sensitive, yet it is not an ideal approach to test the sensitivity of a microfluidic device prototype as well as the optical reader due to the intensive mixing and precise timing requirements. In order to test the device, another approach using Al^{III} determination, which requires less mixing and timing, was first used as a model compound and integrated into the microfluidic device as described in Chapter 4. Evaluation of the performance of the microfluidic device is demonstrated by comparing it to the results generated by a bench-top UV-Vis Spectrometer.

CHAPTER IV A PORTABLE MICROFLUIDIC DEVICE COUPLED WITH A GNP SENSOR FOR ALUMINUM DETECTION

4.1 Introduction

As one of the most widely used metals, aluminum is an element that is often debated about its possible negative heath impacts. Some studies have shown that aluminum can be associated with diseases such as Alzheimer's, dementia, hyperactivity, leaning disorders in children[113] and Parkinson's[109]. Aluminum is found in drinking water sources and treated drinking water[114], food items[115] and ambient air[113]. Migration of aluminum into fluids for human consumption is possible due to direct contact of aluminum-containing packaging[115], thus aluminum alloy for beverage packaging becomes a great concern. In order to limit the potential intake, the WHO has enacted strict guidelines on the level of Al^{III} in drinking water (e.g. 7.4 μM)[95]. Therefore, it is critical to be able to measure the level of Al^{III} in aqueous samples to minimize its intake.

The conventional methods for aluminum detection include graphite furnace atomic absorption spectrometry (GF-AAS)[116], inductively coupled plasma atomic emission spectrometry (ICP-AES)[117], and high-performance ion chromatography with fluorescence detection[118]. However, these methods require bulky and expensive instruments, which is undesired for onsite detection.

Therefore, a simple, selective and sensitive method would be convenient for the detection of Al^{III} for onsite applications.

Gold nanoparticles (GNPs) have been widely applied in many fields, e.g. medical diagnostics[119] and environmental monitoring[16, 47, 100], mainly attributed to their unique surface chemistry and optical properties. Li, et al. [120] described a method utilizing modified GNPs as probes for successful measurement of Al^{III} concentration in aqueous samples, with an LOD of 0.2 μM. In their study, however, the modification of GNPs (via formation of an Au-S bond with a thiol-containing ligand) requires additional procedures, which add to the complexity of the method. Besides, the short half-life of the thiolated GNPs, caused by the rapid decay of the thiol-containing reagent used for functionalization[18], greatly limits the potential for onsite applications. Chen, et al. [109] developed a method with the use of label-free GNPs as probes, which did not require pre-modification of the GNPs, and successfully demonstrated the method for sensitive Al^{III} detection in water samples with an LOD of 1.0 μM. Therefore in our study, the detection of aluminum ions using citrate capped GNPs described by Chen, et al. [109] is adopted.

Microfluidic devices, based on small-scale manipulation of fluids, can be used for medical diagnostics as well as environmental detection of pollutants. Such miniaturization has led to features such as portability, low solvent and

reagent consumption, small sample size, low energy consumption, rapid detection, and very importantly, low cost to build and operate such devices. Detection of many analytes on microfluidic devices including Al^{III} has been demonstrated[121], yet these devices have suffered from some drawbacks such as complicated preparation procedures and operations.

In this study, we demonstrate the use of a low-cost and portable microfluidic device for Al^{III} analysis, yet the device is adaptable for multi-analyte analysis. The key component is an optical reader consisting of an LED array with controllable wavelengths of light, and a corresponding photometer was also developed. This reader is optimal to the optical properties of GNP sensors, such that multi-analytes can be detected with the same reader using different GNPs as probes. A microfluidic chip compatible to this optical reader was fabricated utilizing PDMS and used as a platform for the aluminum assay as described above. The disposable PDMS chip is easy to fabricate and material costs are low. Performance of Al^{III} detection using the device is compared to the conventional approach that requires a bench-top spectrometer.

4.2 Experimental section

4.2.1 GNPs synthesis

The synthesis of GNPs is described in Chapter 3.3.2 in detail. In brief, the classic method for citrate-capped GNPs was adopted[34]. The newly synthesized GNPs were characterized by TEM. The newly synthesized GNP solution was used for the following experiment without any treatment.

4.2.2 PDMS microfluidic chip fabrication and apparatus

The polydimethylsiloxane (PDMS) (SYLGARD R 184) chip was one of the major components and it was placed inside the optical reader (Figure 4.1). It was designed to consist of four sequential chambers as testing zones. An inlet and an outlet were included in the chip for control of the inflow and waste collection, respectively. The channels were 0.5 mm wide and 0.2 mm deep. The chambers were 5 mm by 5 mm and made to have a depth of 0.8 mm, four times the channel depth, to increase the absorbance distance.

The chip was designed in AutoCAD® and fabricated using a mold which was manufactured by Universal Laser Systems VLS2.30 (Scottsdale, U.S.) from plastic transparency sheets. The dry PDMS chip was fixed to the top of a 1" x 3" glass substrate by oxygen-plasma treatment.

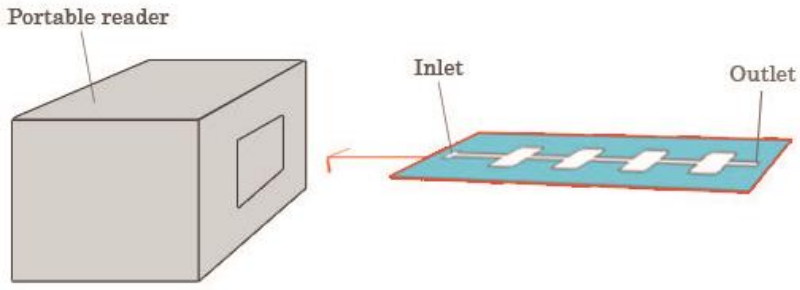

Figure 4.1: Schematic layout of the microfluidic device coupled with the portable optical reader

4.2.3 Optical reader

We have developed an optical reader with the capability of recognizing the optical signals at multiple wavelengths. It also consists of a chamber for use of the microfluidic device. This reader is portable and suitable for many purposes including the detection of heavy metals by GNPs. Due to the consideration of protecting potential intelligent property, the design of the optical reader will not be illustrated in details in this thesis.

4.2.4 Al^{III} detection procedures

The assay was first conducted with a similar setup as discussed in Chapter III using 96-well plates and a bench-top UV-Vis spectrometer. In brief, 150 µl of Al^{III} standard solution was mixed with same volume of a GNP solution (same as the one used in Chapter III without any modification), and scanned by the spectrometer after 10 min. As a consequence, the citrate-capped GNPs were

aggregated by Al^{III} attributed to the high affinity between Al ions and citrate molecules. Then the assay was repeated for detection using the microfluidic device. An aqueous sample of Al^{III} and a GNP solution were first mixed in a microtube by pipetting, and incubated at room temperature for 10 min, followed by the injection of ~20 μL of the assay solution into the microfluidic chip from the inlet using a micro pipette. The chip was then inserted into the optical reader and the readouts were recorded at two wavelengths.

4.3 Results and Discussion

The synthesis and characterization of the GNP solution is described in sections 3.3.1 and 3.4.2, respectively. The GNP sizes were determined to be 15.2 ± 3.6 nm and the solution was highly monodispersed.

4.3.1 Assay results as determined via UV-Vis spectrometry

The spectra of the assays at various Al^{III} concentrations were first recorded to characterize the aggregation of the GNPs induced by Al^{III} (Figure 4.2). As illustrated in the figure (also in Figure 4.3a), after 10-min incubation, the absorbance at 520 nm decreases monotonically as the Al^{III} concentration increases, while the absorbance at 620 nm increases with increasing Al^{III} concentrations and then drops when the concentration is above 6 ppm. In the

process of aggregation, small sizes of particles (SPR peak at ~520 nm) were aggregated to form bigger particles (SPR peak at >520 nm) and thus affecting the colour of the GNP solutions. The number of small particles decreased at a higher rate as the Al concentration increased, and a lower absorbance at 520 nm would be expected. This can explain that the absorbance at 520 nm is inversely proportional to the concentration of Al solution, while directly proportional at 620 nm (when Al ≤ 6 ppm). The reason that the absorbance at 620 nm (and other visible ranges) decreased after the addition of high concentration of Al solution, however, remains unknown. We speculate that the GNP solution start to loss the SPR effect (and colour) when the size of the GNPs reaches a threshold. These trends strongly suggest that the absorbance signal intensity at both 520 and 620 nm can be used for quantification of Al^{III}. Absorbance at both wavelengths were used to construct calibration curves (Figure 4.3b,c). The linear range of absorbance at 520 nm is from 2 – 8 ppm, while that at 620 nm ranges from 1 – 4 ppm linearly. The LOD at 620 nm was calculated to be 1.3 ppm.

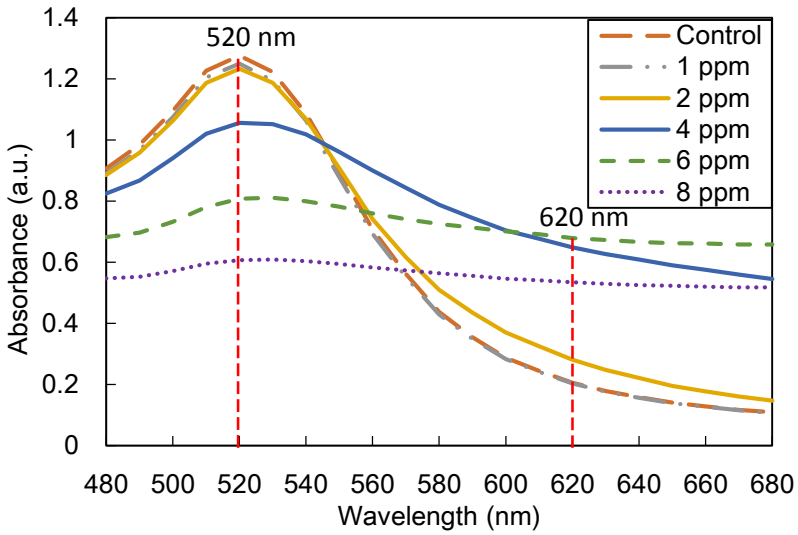

Figure 4.2: The UV-Vis spectra of different samples including the control and a series of Al^{III} standard solutions collected at 10 min. The vertical dashed lines indicate the two wavelengths that are used for the quantification of Al^{III} by UV-Vis and the portable optical reader (515 nm instead of 520 nm).

(a)

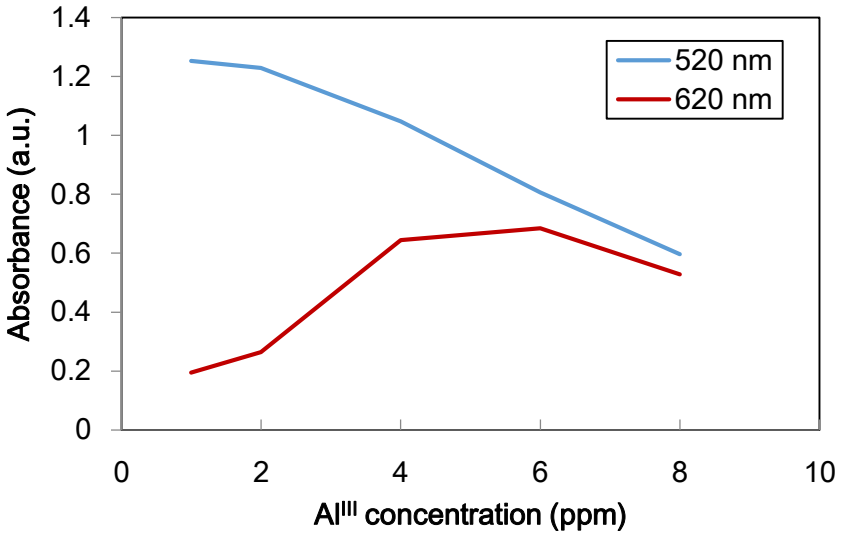

(b)

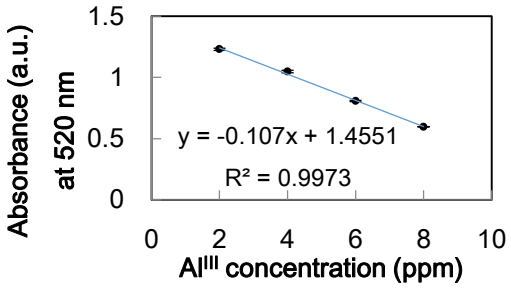

(c)

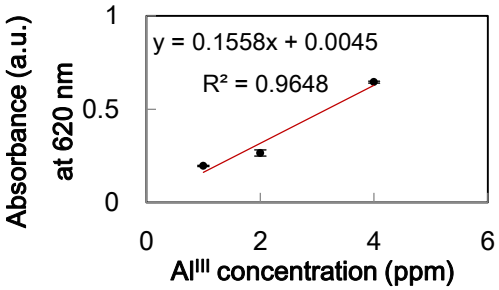

Figure 4.3: (a) The absorbance of various concentrations of Al^{III} standard solutions at 10 min determined by UV-Vis Spec; (b) and (c) the calibration curves using the absorbance at 520 nm and 620 nm, respectively, based on four replicates with the error bars representing standard deviations.

4.3.2 Performance of the microfluidic device

The assay was then tested on the microfluidic device coupled with the optical reader described in section 4.2.3. The data were analyzed in a similar way and compared with those collected from UV-Vis spectrometry for the evaluation of

device performance. The results show similar trends and similar LOD was achieved, indicating the high sensitivity of the microfluidic device to detect the colour change of the GNP probes. The detailed results will not be described here to protect the potential intelligent properties.

One significant advantage of the device is that the wavelengths of the light source are controllable and can be easily adjusted to the desired range of the surface plasmon resonance (SPR) of GNP probes. Moreover, the microfluidic chip is disposable and is designed to have 4 detection zones or more for high throughput detections (not yet demonstrated in this study).

Considering that the light path in the microfluidic device in this study is only 0.8 mm, which is much less than that of the 96-well plate used for UV-Vis Spec measurements (1 cm), an increase in depth of the detection zone would consequentially increase the light distance through the sample, contributing to a higher sensitivity. This can be done by either fabricating a thicker detection zone for the microfluidic chips or by switching the light direction from vertical to horizontal. In addition, the assay can be further optimized by finely tuning the pH of the GNP solutions to replicate the LOD (1 μM, or 27 ppb) described by Chen, et al. [109], such that the GNP probes can be used in a microfluidic device for onsite applications. Additionally, one may notice that the method described in Chapter 3 shares similar mechanisms for quantifying Pb^{II} by using the

absorbance at both 520 nm and 610 nm, indicating the potential use of the same device for multi-analyte detection. Moreover, a more advanced design with a passive mixer integrated into the microfluidic chip will be realized in the near future and thus no pre-mixing will be required.

4.4 Conclusion

We have successfully developed a simple and sensitive device prototype for quantitative determination of Al^{III} and potentially for other metal ions (not yet demonstrated in this study) by GNP probes in aqueous solutions. The performance of the device is comparable with UV-Vis Spec for Al^{III} detection. The device is designed to be capable of analyzing multiple metal analytes. Operation of the device is simple as only pipetting is required. The LOD is expected to be greatly improved by a few proposed solutions, including increasing the light path and optimizing the chemical assay. This device provides a promising application for onsite analysis of metal ions in water.

CHAPTER V SUMMARY AND CONCLUSIONS

In this study, a rapid and simple label-free assay using GNPs for sensitive Pb^{II} detection in water has been demonstrated without the use of corrosive or hazardous agents. Compared to other assays using GNPs for metal ion detection in the literature, our approach is simplified by eliminating the need to modify the GNPs, and therefore has a greater potential for field applications. Non-modified GNPs are stable at room temperature for an extended period of time compared to modified GNPs. The LOD of this assay conducted using DI water spiked with Pb^{II} was 6.0 ppb, lower than the WHO limit for drinking water of 10 ppb. The current assay with a detection time of 10 min has a linear dynamic range from the LOD up to ~500 ppb. The detection can be easily realized using a spectrometer. A future study to minimize the impact of interfering ions may bring the assay much closer to real world applications.

A simple and sensitive microfluidic device prototype for quantitative determination of Al^{III} by GNP probes in aqueous solutions has been fabricated. This device shows comparable LOD (1.2 ppm) with that of a UV-Vis Spec (1.3 ppm) with 96-well plate and is designed to be capable of multi-analyte analysis. Operation of the device is simple as only pipetting is required. The LOD is expected to be greatly improved by several proposals, especially optimizing the

chemical assay, and such improvements are is progress. This device is promising for onsite analysis of metal ions in water.

LIST OF REFERENCES

1. Aragay, G.; Pons, J.; Merkoçi, A., Recent trends in macro-, micro-, and nanomaterial-based tools and strategies for heavy-metal detection. *Chemical Reviews* **2011,** *111* (5), 3433-3458.

2. Health Canada *Final human health state of the science report on Lead*; 2013, http://www.hc-sc.gc.ca/ewh-semt/pubs/contaminants/dhhssrl-rpecscepsh/index-eng.php, Accessed on July 17, 2013.

3. Health Canada *Guidelines for Canadian drinking water quality summary table*; 2012, http://www.hc-sc.gc.ca/ewh-semt/pubs/water-eau/2012-sum_guide-res_recom/index-eng.php, Accessed on July 17, 2013.

4. Health Canada *Lead*; 1992, http://www.hc-sc.gc.ca/ewh-semt/pubs/water-eau/lead-plomb/index-eng.php, Accessed on July 17, 2013.

5. Xia, N.; Shi, Y.; Zhang, R.; Zhao, F.; Liu, F.; Liu, L., Simple, rapid and label-free colorimetric assay for arsenic based on unmodified gold nanoparticles and a phytochelatin-like peptide. *Analytical Methods* **2012,** *4* (12), 3937-3941.

6. Anran, G.; Xiang, L.; Tie, L.; Ping, Z.; Yuelin, W.; Qing, Y.; Lihua, W.; Chunhai, F., Digital microfluidic chip for rapid portable detection of Mercury(II). *Sensors Journal, IEEE* **2011,** *11* (11), 2820-2824.

7. Hu, M.; Chen, J.; Li, Z.-Y.; Au, L.; Hartland, G. V.; Li, X.; Marquez, M.; Xia, Y., Gold nanostructures: engineering their plasmonic properties for biomedical applications. *Chemical Society Reviews* **2006,** *35* (11), 1084-1094.

8. Wang, Z.; Lu, Y., Functional DNA directed assembly of nanomaterials for biosensing. *Journal of Materials Chemistry* **2009,** *19* (13), 1788-1798.

9. Liu, J.; Lu, Y., Adenosine-dependent assembly of aptazyme-functionalized gold nanoparticles and its application as a colorimetric biosensor. *Analytical Chemistry* **2004,** *76* (6), 1627-1632.

10. Sudeep, P. K.; Joseph, S. T. S.; Thomas, K. G., Selective detection of cysteine and glutathione using gold nanorods. *Journal of the American Chemical Society* **2005,** *127* (18), 6516-6517.

11. (a) Xue, X.; Wang, F.; Liu, X., One-step, room temperature, colorimetric detection of mercury (Hg2+) using DNA/nanoparticle conjugates. *Journal of the American Chemical Society* **2008,** *130* (11), 3244-3245; (b) Darbha, G. K.; Ray, A.; Ray, P. C.,

Gold nanoparticle-based miniaturized nanomaterial surface energy transfer probe for rapid and ultrasensitive detection of mercury in soil, water, and fish. *ACS Nano* **2007,** *1* (3), 208-214.

12. Toma, H. E.; Zamarion, V. M.; Toma, S. H.; Araki, K., The coordination chemistry at gold nanoparticles. *Journal of the Brazilian Chemical Society* **2010,** *21*, 1158-1176.

13. Daniel, M.-C.; Astruc, D., Gold nanoparticles: Assembly, supramolecular chemistry, quantum-size-related properties, and applications toward biology, catalysis, and nanotechnology. *Chemical Reviews* **2003,** *104* (1), 293-346.

14. DeLong, R. K.; Reynolds, C. M.; Malcolm, Y.; Schaeffer, A.; Severs, T.; Wanekaya, A., Functionalized gold nanoparticles for the binding, stabilization, and delivery of therapeutic DNA, RNA, and other biological macromolecules. *Nanotechnology, Science and Applications* **2010,** *2010:3*, 53 - 63.

15. Kalluri, J. R.; Arbneshi, T.; Afrin Khan, S.; Neely, A.; Candice, P.; Varisli, B.; Washington, M.; McAfee, S.; Robinson, B.; Banerjee, S.; Singh, A. K.; Senapati, D.; Ray, P. C., Use of gold nanoparticles in a simple colorimetric and ultrasensitive dynamic light scattering assay: Selective detection of arsenic in groundwater. *Angewandte Chemie International Edition* **2009,** *48* (51), 9668-9671.

16. Darbha, G. K.; Singh, A. K.; Rai, U. S.; Yu, E.; Yu, H.; Chandra Ray, P., Selective detection of mercury (II) ion using nonlinear optical properties of gold nanoparticles. *Journal of the American Chemical Society* **2008,** *130* (25), 8038-8043.

17. (a) Chai, F.; Wang, C.; Wang, T.; Li, L.; Su, Z., Colorimetric detection of Pb2+ using glutathione functionalized gold nanoparticles. *ACS Applied Materials & Interfaces* **2010,** *2* (5), 1466-1470; (b) Huang, K.-W.; Yu, C.-J.; Tseng, W.-L., Sensitivity enhancement in the colorimetric detection of lead(II) ion using gallic acid–capped gold nanoparticles: Improving size distribution and minimizing interparticle repulsion. *Biosensors and Bioelectronics* **2010,** *25* (5), 984-989; (c) Beqa, L.; Singh, A. K.; Khan, S. A.; Senapati, D.; Arumugam, S. R.; Ray, P. C., Gold nanoparticle-based simple colorimetric and ultrasensitive dynamic light scattering assay for the selective detection of Pb(II) from paints, plastics, and water samples. *ACS Applied Materials & Interfaces* **2011,** *3* (3), 668-673.

18. Stevens, R.; Stevens, L.; Price, N. C., The stabilities of various thiol compounds used in protein purifications. *Biochemical Education* **1983,** *11* (2), 70-70.

19. Templeton, A. C.; Wuelfing, W. P.; Murray, R. W., Monolayer-protected cluster molecules. *Accounts of Chemical Research* **1999,** *33* (1), 27-36.
20. Li, W.; Nie, Z.; He, K.; Xu, X.; Li, Y.; Huang, Y.; Yao, S., Simple, rapid and label-free colorimetric assay for Zn2+ based on unmodified gold nanoparticles and specific Zn2+ binding peptide. *Chemical Communications* **2011,** *47* (15), 4412-4414.
21. Kim, P.; Kwon, K. W.; Park, M. C.; Lee, S. H.; Kim, S. M.; Suh, K. Y., *Soft lithography for microfluidics: A review*. 2008.
22. (a) McDonald, J. C.; Duffy, D. C.; Anderson, J. R.; Chiu, D. T.; Wu, H.; Schueller, O. J. A.; Whitesides, G. M., Fabrication of microfluidic systems in poly(dimethylsiloxane). *Electrophoresis* **2000,** *21* (1), 27-40; (b) Wu, J.; Gu, M., Microfluidic sensing: state of the art fabrication and detection techniques. *Journal of Biomedical Optics* **2011,** *16* (8), 080901-080901.
23. Fiorini, G. S.; Chiu, D. T., Disposable microfluidic devices: fabrication, function, and application. *BioTechniques* **2005,** *38* (3), 429-446.
24. McDonald Jc, W. G. M., Poly(dimethylsiloxane) as a material for fabricating microfluidic devices. *Accounts of Chemical Research* **2002,** *35* (7), 491-9.
25. Sia Sk, W. G. M., Microfluidic devices fabricated in poly(dimethylsiloxane) for biological studies. *Electrophoresis* **2003,** *24* (21), 3563-76.
26. Benazzi, G.; Holmes, D.; Sun, T.; Mowlem, M. C.; Morgan, H., Discrimination and analysis of phytoplankton using a microfluidic cytometer. *Nanobiotechnology, IET* **2007,** *1* (6), 94-101.
27. Jing, G.; Polaczyk, A.; Oerther, D. B.; Papautsky, I., Development of a microfluidic biosensor for detection of environmental mycobacteria. *Sensors and Actuators B: Chemical* **2007,** *123* (1), 614-621.
28. Malecha, K.; Pijanowska, D. G.; Golonka, L. J.; Torbicz, W., LTCC microreactor for urea determination in biological fluids. *Sensors and Actuators B: Chemical* **2009,** *141* (1), 301-308.
29. Noblitt, S. D.; Lewis, G. S.; Liu, Y.; Hering, S. V.; Collett, J. L.; Henry, C. S., Interfacing microchip electrophoresis to a growth tube particle collector for semicontinuous monitoring of aerosol composition. *Analytical Chemistry* **2009,** *81* (24), 10029-10037.
30. (a) Chang, I.-H.; Tulock, J. J.; Liu, J.; Kim, W.-S.; Cannon, D. M.; Lu, Y.; Bohn, P. W.; Sweedler, J. V.; Cropek, D. M., Miniaturized lead sensor based on lead-specific

DNAzyme in a nanocapillary interconnected microfluidic device. *Environmental Science & Technology* **2005,** *39* (10), 3756-3761; (b) Nuriman; Kuswandi, B.; Verboom, W., Optical fiber chemical sensing of Hg(II) ions in aqueous samples using a microfluidic device containing a selective tripodal chromoionophore-PVC film. *Sensors and Actuators B: Chemical* **2011,** *157* (2), 438-443; (c) Alves-Segundo, R.; Ibañez-Garcia, N.; Baeza, M.; Puyol, M.; Alonso-Chamarro, J., Towards a monolithically integrated microsystem based on the green tape ceramics technology for spectrophotometric measurements. Determination of chromium (VI) in water. *Microchim Acta* **2011,** *172* (1-2), 225-232.

31. García-Alonso, J.; Greenway, G. M.; Hardege, J. D.; Haswell, S. J., A prototype microfluidic chip using fluorescent yeast for detection of toxic compounds. *Biosensors and Bioelectronics* **2009,** *24* (5), 1508-1511.

32. He, S.; Li, D.; Zhu, C.; Song, S.; Wang, L.; Long, Y.; Fan, C., Design of a gold nanoprobe for rapid and portable mercury detection with the naked eye. *Chemical Communications* **2008,** *0* (40), 4885-4887.

33. Date, Y.; Terakado, S.; Sasaki, K.; Aota, A.; Matsumoto, N.; Shiku, H.; Ino, K.; Watanabe, Y.; Matsue, T.; Ohmura, N., Microfluidic heavy metal immunoassay based on absorbance measurement. *Biosensors and Bioelectronics* **2012,** *33* (1), 106-112.

34. (a) Turkevich, J.; Stevenson, P. C.; Hillier, J., A study of the nucleation and growth processes in the synthesis of colloidal gold. *Discussions of the Faraday Society* **1951,** *11* (0), 55-75; (b) G., F., Controlled nucleation for the regulation of the particle size in monodisperse gold suspensions. *Nature Physical Science* **1973,** *241*, 20-22.

35. Liu, J.; Lu, Y., Preparation of aptamer-linked gold nanoparticle purple aggregates for colorimetric sensing of analytes. *Nat. Protocols* **2006,** *1* (1), 246-252.

36. Hutchinson, T. C. M. K. M. I. C. o. S. U. S. C. o. P. o. t. E., *Lead, mercury, cadmium, and arsenic in the environment*. Published on behalf of the Scientific Committee on Problems of the Environment (Scope) of the International Council of Scientific Unions by (ICSU) Wiley: Chichester; New York, 1987.

37. Rose, M.; Knaggs, M.; Owen, L.; Baxter, M., A review of analytical methods for lead, cadmium, mercury, arsenic and tin determination used in proficiency testing. *Journal of Analytical Atomic Spectrometry* **2001,** *16* (9), 1101-1106.

38. (a) Marle, L.; Greenway, G. M., Microfluidic devices for environmental monitoring. *TrAC Trends in Analytical Chemistry* **2005,** *24* (9), 795-802; (b) Jang, A.; Zou, Z.; Lee, K.

K.; Ahn, C. H.; Bishop, P. L., State-of-the-art lab chip sensors for environmental water monitoring. *Measurement Science and Technology* **2011,** *22* (3).

39. (a) Dittrich, P. S.; Tachikawa, K.; Manz, A., Micro total analysis systems. Latest advancements and trends. *Analytical Chemistry* **2006,** *78* (12), 3887-3908; (b) Manz, A.; Graber, N.; Widmer, H. M., Miniaturized total chemical analysis systems: A novel concept for chemical sensing. *Sensors and Actuators B: Chemical* **1990,** *1* (1–6), 244-248.

40. Pumera, M.; Merkoçi, A.; Alegret, S., New materials for electrochemical sensing VII. Microfluidic chip platforms. *TrAC Trends in Analytical Chemistry* **2006,** *25* (3), 219-235.

41. (a) Johnson, R. D.; Gavalas, V. G.; Daunert, S.; Bachas, L. G., Microfluidic ion-sensing devices. *Analytica Chimica Acta* **2008,** *613* (1), 20-30; (b) Li, H.-F.; Lin, J.-M., Applications of microfluidic systems in environmental analysis. *Anal Bioanal Chem* **2009,** *393* (2), 555-567.

42. Jaffrezic-Renault, N.; Dzyadevych, S., Conductometric microbiosensors for environmental monitoring. *Sensors* **2008,** *8* (4), 2569-2588.

43. Verma, N.; Singh, M., Biosensors for heavy metals. *Biometals* **2005,** *18* (2), 121-129.

44. Li, M.; Gou, H.; Al-Ogaidi, I.; Wu, N., Nanostructured sensors for detection of heavy metals: A review. *ACS Sustainable Chemistry & Engineering* **2013**.

45. Jokerst, J. C.; Emory, J. M.; Henry, C. S., Advances in microfluidics for environmental analysis. *Analyst* **2012,** *137* (1), 24-34.

46. Yuan, M.; Zhu, Y.; Lou, X.; Chen, C.; Wei, G.; Lan, M.; Zhao, J., Sensitive label-free oligonucleotide-based microfluidic detection of mercury (II) ion by using exonuclease I. *Biosensors and Bioelectronics* **2012,** *31* (1), 330-336.

47. Zhang, M.; Liu, Y.-Q.; Ye, B.-C., Colorimetric assay for parallel detection of Cd2+, Ni2+ and Co2+ using peptide-modified gold nanoparticles. *Analyst* **2012,** *137* (3), 601-607.

48. Zhang, M.; Ge, L.; Ge, S.; Yan, M.; Yu, J.; Huang, J.; Liu, S., Three-dimensional paper-based electrochemiluminescence device for simultaneous detection of Pb2+ and Hg2+ based on potential-control technique. *Biosensors and Bioelectronics* **2013,** *41* (0), 544-550.

49. Ono, A.; Togashi, H., Highly selective oligonucleotide-based sensor for mercury(II) in aqueous solutions. *Angewandte Chemie International Edition* **2004,** *43* (33), 4300-4302.
50. Ng, J. M. K.; Gitlin, I.; Stroock, A. D.; Whitesides, G. M., Components for integrated poly(dimethylsiloxane) microfluidic systems. *Electrophoresis* **2002,** *23* (20), 3461-3473.
51. Breaker, R. R.; Joyce, G. F., A DNA enzyme that cleaves RNA. *Chemistry & Biology* **1994,** *1* (4), 223-229.
52. Woese, C. R., *The genetic code : the molecular basis for genetic expression*. Harper & Row: New York, 1967.
53. Li, J.; Lu, Y., A highly sensitive and selective catalytic DNA biosensor for lead ions. *Journal of the American Chemical Society* **2000,** *122* (42), 10466-10467.
54. Liu, J.; Lu, Y., Improving fluorescent DNAzyme biosensors by combining inter- and intramolecular quenchers. *Analytical Chemistry* **2003,** *75* (23), 6666-6672.
55. Chao, C.-H.; Wu, C.-S.; Huang, C.-C.; Liang, J.-C.; Wang, H.-T.; Tang, P.-T.; Lin, L.-Y.; Ko, F.-H., A rapid and portable sensor based on protein-modified gold nanoparticle probes and lateral flow assay for naked eye detection of mercury ion. *Microelectronic Engineering* **2012,** *97* (0), 294-296.
56. Date, Y.; Aota, A.; Terakado, S.; Sasaki, K.; Matsumoto, N.; Watanabe, Y.; Matsue, T.; Ohmura, N., Trace-leve mercury ion (Hg2+) analysis in aqueous sample based on solid-phase extraction followed by microfluidic immunoassay. *Analytical Chemistry* **2012,** *85* (1), 434-440.
57. Buffi, N.; Merulla, D.; Beutier, J.; Barbaud, F.; Beggah, S.; van Lintel, H.; Renaud, P.; Roelof van der Meer, J., Development of a microfluidics biosensor for agarose-bead immobilized Escherichia coli bioreporter cells for arsenite detection in aqueous samples. *Lab on a Chip* **2011,** *11* (14), 2369-2377.
58. Date, A.; Pasini, P.; Sangal, A.; Daunert, S., Packaging sensing cells in spores for long-term preservation of sensors: a tool for biomedical and environmental analysis. *Analytical Chemistry* **2010,** *82* (14), 6098-6103.
59. Rothert, A.; Deo, S. K.; Millner, L.; Puckett, L. G.; Madou, M. J.; Daunert, S., Whole-cell-reporter-gene-based biosensing systems on a compact disk microfluidics platform. *Analytical Biochemistry* **2005,** *342* (1), 11-19.

60. Prindle, A.; Samayoa, P.; Razinkov, I.; Danino, T.; Tsimring, L. S.; Hasty, J., A sensing array of radically coupled genetic /`biopixels/'. *Nature* **2012,** *481* (7379), 39-44.
61. Date, A.; Pasini, P.; Daunert, S., Integration of spore-based genetically engineered whole-cell sensing systems into portable centrifugal microfluidic platforms. *Anal Bioanal Chem* **2010,** *398* (1), 349-356.
62. Diesel, E.; Schreiber, M.; Meer, J., Development of bacteria-based bioassays for arsenic detection in natural waters. *Anal Bioanal Chem* **2009,** *394* (3), 687-693.
63. U.S. Environmental Protection Agency, National primary drinking water regulations. **2009**.
64. (a) Lee, M. H.; Wu, J.-S.; Lee, J. W.; Jung, J. H.; Kim, J. S., Highly sensitive and selective chemosensor for Hg2+ based on the rhodamine fluorophore. *Organic Letters* **2007,** *9* (13), 2501-2504; (b) Wu, F.-Y.; Bae, S. W.; Hong, J.-I., A selective fluorescent sensor for Pb(II) in water. *Tetrahedron Letters* **2006,** *47* (50), 8851-8854; (c) Peng, X.; Du, J.; Fan, J.; Wang, J.; Wu, Y.; Zhao, J.; Sun, S.; Xu, T., A selective fluorescent sensor for imaging Cd2+ in living cells. *Journal of the American Chemical Society* **2007,** *129* (6), 1500-1501; (d) Métivier, R.; Leray, I.; Valeur, B., Lead and mercury sensing by calixarene-based fluoroionophores bearing two or four dansyl fluorophores. *Chemistry – A European Journal* **2004,** *10* (18), 4480-4490; (e) Nuriman; Kuswandi, B.; Verboom, W., Selective chemosensor for Hg(II) ions based on tris[2-(4-phenyldiazenyl)phenylaminoethoxy]cyclotriveratrylene in aqueous samples. *Analytica Chimica Acta* **2009,** *655* (1–2), 75-79; (f) Som-aum, W.; Li, H.; Liu, J.; Lin, J.-M., Determination of arsenate by sorption pre-concentration on polystyrene beads packed in a microfluidic device with chemiluminescence detection. *Analyst* **2008,** *133* (9), 1169-1175; (g) Faye, D.; Zhang, H.; Lefevre, J.-P.; Bell, J.; Delaire, J. A.; Leray, I., Mercury detection in a microfluidic device by using a molecular sensor soluble in organoaqueous solvent. *Photochemical & Photobiological Sciences* **2012,** *11* (11), 1737-1743.
65. (a) Kou, S.; Nam, S.-W.; Shumi, W.; Lee, M.-H.; Bae, S.-W.; Du, J.; Kim, J.-S.; Hong, J.-I.; Peng, X.; Yoon, J.-Y.; Park, S.-S., Microfluidic detection of multiple heavy metal ions using fluorescent chemosensors. *Bulletin of the Korean Chemical Society* **2009,** *30* (5), 1173-1176; (b) Zhao, L.; Wu, T.; Lefevre, J.-P.; Leray, I.; Delaire, J. A., Fluorimetric lead detection in a microfluidic device. *Lab on a Chip* **2009,** *9* (19), 2818-2823.

66. LaCroix-Fralish, A.; Clare, J.; Skinner, C. D.; Salin, E. D., A centrifugal microanalysis system for the determination of nitrite and hexavalent chromium. *Talanta* **2009,** *80* (2), 670-675.

67. Fan, C.; He, S.; Liu, G.; Wang, L.; Song, S., A portable and power-free microfluidic device for rapid and sensitive lead (Pb2+) detection. *Sensors* **2012,** *12* (7), 9467-9475.

68. Zhang, H.; Faye, D.; Lefèvre, J.-P.; Delaire, J. A.; Leray, I., Selective fluorimetric detection of cadmium in a microfluidic device. *Microchemical Journal* **2013,** *106* (0), 167-173.

69. Sawyer, C. N.; McCarty, P. L.; Parkin, G. F., Chemistry for environmental engineering, 4th Ed. *McGraw-Hill* **1994**, 74-79.

70. Palchetti, I.; Marrazza, G.; Mascini, M., New procedures to obtain electrochemical sensors for heavy metal detection. *Analytical Letters* **2001,** *34* (6), 813-824.

71. (a) Palchetti, I.; Cagnini, A.; Mascini, M.; Turner, A. P. F., Characterisation of screen-printed electrodes for detection of heavy metals. *Microchim Acta* **1999,** *131* (1-2), 65-73; (b) Wang, J.; Lu, J.; Hocevar, S. B.; Farias, P. A.; Ogorevc, B., Bismuth-coated carbon electrodes for anodic stripping voltammetry. *Anal Chem* **2000,** *72* (14), 3218-22; (c) Laschi, S.; Palchetti, I.; Mascini, M., Gold-based screen-printed sensor for detection of trace lead. *Sensors and Actuators B: Chemical* **2006,** *114* (1), 460-465; (d) Morton, J.; Havens, N.; Mugweru, A.; Wanekaya, A. K., Detection of trace heavy metal ions using carbon nanotube- modified electrodes. *Electroanalysis* **2009,** *21* (14), 1597-1603.

72. (a) Zhou, J.; Ren, K.; Zheng, Y.; Su, J.; Zhao, Y.; Ryan, D.; Wu, H., Fabrication of a microfluidic Ag/AgCl reference electrode and its application for portable and disposable electrochemical microchips. *Electrophoresis* **2010,** *31* (18), 3083-3089; (b) Shi, J.; Tang, F.; Xing, H.; Zheng, H.; Lianhua, B.; Wei, W., Electrochemical detection of Pb and Cd in paper-based microfluidic devices. *Journal of the Brazilian Chemical Society* **2012,** *23*, 1124-1130.

73. Chen, G.; Lin, Y.; Wang, J., Monitoring environmental pollutants by microchip capillary electrophoresis with electrochemical detection. *Talanta* **2006,** *68* (3), 497-503.

74. Yun, K.-S. K. H.-J. J. S. K. J. Y. E., Analysis of heavy-metal ions using mercury microelectrodes and a solid-state reference electrode on a Si wafer. *Jpn. J. Appl. Phys. Japanese Journal of Applied Physics* **2000,** *39* (Part 1, No. 12B), 7159-7163.

75. Wang, J., Stripping analysis at Bismuth electrodes: A review. *Electroanalysis* **2005,** *17* (15-16), 1341-1346.
76. Hočevar, S. B.; Švancara, I.; Vytřas, K.; Ogorevc, B., Novel electrode for electrochemical stripping analysis based on carbon paste modified with bismuth powder. *Electrochimica Acta* **2005,** *51* (4), 706-710.
77. Jothimuthu, P.; Wilson, R.; Herren, J.; Haynes, E.; Heineman, W.; Papautsky, I., Lab-on-a-chip sensor for detection of highly electronegative heavy metals by anodic stripping voltammetry. *Biomed Microdevices* **2011,** *13* (4), 695-703.
78. Jung, W.; Jang, A.; Bishop, P. L.; Ahn, C. H., A polymer lab chip sensor with microfabricated planar silver electrode for continuous and on-site heavy metal measurement. *Sensors and Actuators B: Chemical* **2011,** *155* (1), 145-153.
79. Nie, Z.; Nijhuis, C. A.; Gong, J.; Chen, X.; Kumachev, A.; Martinez, A. W.; Narovlyansky, M.; Whitesides, G. M., Electrochemical sensing in paper-based microfluidic devices. *Lab on a Chip* **2010,** *10* (4), 477-483.
80. Fytianos, K., Speciation analysis of heavy metals in natural waters: a review. *Journal of AOAC International* **2001,** *84* (6), 1763-1769.
81. Chen, Y.; Rosenzweig, Z., Luminescent CdS quantum dots as selective ion probes. *Analytical Chemistry* **2002,** *74* (19), 5132-5138.
82. (a) Wang, Z.; Lee, J. H.; Lu, Y., Label-free colorimetric detection of Lead ions with a nanomolar detection limit and tunable dynamic range by using gold nanoparticles and DNAzyme. *Advanced Materials* **2008,** *20* (17), 3263-3267; (b) Xu, Y.; Deng, L.; Wang, H.; Ouyang, X.; Zheng, J.; Li, J.; Yang, R., Metal-induced aggregation of mononucleotides-stabilized gold nanoparticles: an efficient approach for simple and rapid colorimetric detection of Hg(ii). *Chemical Communications* **2011,** *47* (21), 6039-6041; (c) He, X.; Liu, H.; Li, Y.; Wang, S.; Li, Y.; Wang, N.; Xiao, J.; Xu, X.; Zhu, D., Gold nanoparticle-based fluorometric and colorimetric sensing of Copper(II) Ions. *Advanced Materials* **2005,** *17* (23), 2811-2815.
83. Martinez, A. W.; Phillips, S. T.; Nie, Z.; Cheng, C.-M.; Carrilho, E.; Wiley, B. J.; Whitesides, G. M., Programmable diagnostic devices made from paper and tape. *Lab on a Chip* **2010,** *10* (19), 2499-2504.
84. Carrilho, E.; Martinez, A. W.; Whitesides, G. M., Understanding wax printing: A simple micropatterning process for paper-based microfluidics. *Analytical Chemistry* **2009,** *81* (16), 7091-7095.

85. Yan, Q.; Peng, B.; Su, G.; Cohan, B. E.; Major, T. C.; Meyerhoff, M. E., Measurement of tear glucose levels with amperometric glucose biosensor/capillary tube configuration. *Analytical Chemistry* **2011,** *83* (21), 8341-8346.
86. Ellerbee, A. K.; Phillips, S. T.; Siegel, A. C.; Mirica, K. A.; Martinez, A. W.; Striehl, P.; Jain, N.; Prentiss, M.; Whitesides, G. M., Quantifying colorimetric assays in paper-based microfluidic devices by measuring the transmission of light through paper. *Analytical Chemistry* **2009,** *81* (20), 8447-8452.
87. (a) Cheng, C.-M.; Martinez, A. W.; Gong, J.; Mace, C. R.; Phillips, S. T.; Carrilho, E.; Mirica, K. A.; Whitesides, G. M., Paper-based ELISA. *Angewandte Chemie International Edition* **2010,** *49* (28), 4771-4774; (b) Liu, X. Y.; Cheng, C. M.; Martinez, A. W.; Mirica, K. A.; Li, X. J.; Phillips, S. T.; Mascaren; x; as, M.; Whitesides, G. M. In *A portable microfluidic paper-based device for ELISA*, Micro Electro Mechanical Systems (MEMS), 2011 IEEE 24th International Conference on, 23-27 Jan. 2011; 2011; pp 75-78.
88. (a) Ornatska, M.; Sharpe, E.; Andreescu, D.; Andreescu, S., Paper bioassay based on ceria nanoparticles as colorimetric probes. *Analytical Chemistry* **2011,** *83* (11), 4273-4280; (b) Xiang, Y.; Lu, Y., Using personal glucose meters and functional DNA sensors to quantify a variety of analytical targets. *Nat Chem* **2011,** *3* (9), 697-703.
89. (a) Govindarajan, A. V.; Ramachandran, S.; Vigil, G. D.; Yager, P.; Bohringer, K. F. In *Microfluidic origami for point-of-care extraction of nucleic acids from viscous samples*, Micro Electro Mechanical Systems (MEMS), 2011 IEEE 24th International Conference on, 23-27 Jan. 2011; 2011; pp 932-935; (b) Liu, H.; Crooks, R. M., Three-dimensional paper microfluidic devices assembled using the principles of origami. *Journal of the American Chemical Society* **2011,** *133* (44), 17564-17566; (c) Martinez, A. W.; Phillips, S. T.; Carrilho, E.; Thomas, S. W.; Sindi, H.; Whitesides, G. M., Simple telemedicine for developing regions: Camera phones and paper-based microfluidic devices for real-Time, off-site diagnosis. *Analytical Chemistry* **2008,** *80* (10), 3699-3707.
90. Nie, Z.; Deiss, F.; Liu, X.; Akbulut, O.; Whitesides, G. M., Integration of paper-based microfluidic devices with commercial electrochemical readers. *Lab on a Chip* **2010,** *10* (22), 3163-3169.
91. Chin, C. D.; Cheung, Y. K.; Laksanasopin, T.; Modena, M. M.; Chin, S. Y.; Sridhara, A. A.; Steinmiller, D.; Linder, V.; Mushingantahe, J.; Umviligihozo, G.; Karita, E.; Mwambarangwe, L.; Braunstein, S. L.; van de Wijgert, J.; Sahabo, R.; Justman, J. E.;

El-Sadr, W.; Sia, S. K., Mobile device for disease diagnosis and data tracking in resource-limited settings. *Clinical Chemistry* **2013,** *59* (4), 629-640.

92. Madejón P, M. J. M. M. T. C. F. L. R., Bioaccumulation of As, Cd, Cu, Fe and Pb in wild grasses affected by the Aznalcóllar mine spill (SW Spain). *The Science of the total environment* **2002,** *290* (1-3), 1-3.

93. Needleman, H. L.; Gunnoe, C.; Leviton, A.; Reed, R.; Peresie, H.; Maher, C.; Barrett, P., Deficits in psychologic and classroom performance of children with elevated dentine lead levels. *New England Journal of Medicine* **1979,** *300* (13), 689-695.

94. Bowen, W. H., Exposure to metal ions and susceptibility to dental caries. *Journal of dental education* **2001,** *65* (10), 1046-53.

95. World Health Organization, *Guidelines for drinking-water quality*. 3rd ed.; 2008; Vol. 1.

96. (a) Guidotti, T. L.; Calhoun, T.; Davies-Cole, J. O.; Knuckles, M. E.; Stokes, L.; Glymph, C.; Lum, G.; Moses, M. S.; Goldsmith, D. F.; Ragain, L., *Elevated lead in drinking water in Washington, DC, 2003-2004 : The public health response*. US Department of Health and Human Services: Research Triangle Park, NC, ETATS-UNIS, 2007; Vol. 115, p 7; (b) U.S. Environmental Protection Agency *Elevated Lead in D.C. Drinking Water: A Study of Potential Causative Events*; EPA 810-F-07-002; 2007, Accessed on Aug. 9, 2013.

97. Amendola, V.; Meneghetti, M., Size evaluation of gold nanoparticles by UV−vis spectroscopy. *The Journal of Physical Chemistry C* **2009,** *113* (11), 4277-4285.

98. Huang, X.; Jain, P. K.; El-Sayed, I. H.; El-Sayed, M. A., Gold nanoparticles: interesting optical properties and recent applications in cancer diagnostics and therapy. *Nanomedicine (London, England)* **2007,** *2* (5), 681-93.

99. Bao, Q.-Y.; Geng, D.-D.; Xue, J.-W.; Zhou, G.; Gu, S.-Y.; Ding, Y.; Zhang, C., Glutathione-mediated drug release from Tiopronin-conjugated gold nanoparticles for acute liver injury therapy. *International Journal of Pharmaceutics* **2013,** *446* (1–2), 112-118.

100. Huang, D.; Niu, C.; Ruan, M.; Wang, X.; Zeng, G.; Deng, C., Highly sensitive strategy for Hg2+ detection in environmental water samples using long lifetime fluorescence quantum dots and gold nanoparticles. *Environmental Science & Technology* **2013,** *47* (9), 4392-4398.

101. Hui, W.; Bingling, L.; Jing, L.; Shaojun, D.; Erkang, W., DNAzyme-based colorimetric sensing of lead (Pb 2+) using unmodified gold nanoparticle probes. *Nanotechnology* **2008,** *19* (9), 095501.
102. Mao, X.; Li, Z.-P.; Tang, Z.-Y., One pot synthesis of monodispersed L-glutathione stabilized gold nanoparticles for the detection of Pb2+ ions. *Front. Mater. Sci.* **2011,** *5* (3), 322-328.
103. (a) Anwar, Z. M., *Complexation equilibria of Zn(II), Pb(II) and Cd(II) with reduced glutathione (GSH) and biologically important zwitterionic buffers*. Chemical Society: Taipei, TAIWAN, PROVINCE DE CHINE, 2005; Vol. 52, p 9; (b) Krezel, A.; Bal, W., Coordination chemistry of glutathione. *Acta biochimica Polonica* **1999,** *46* (3), 567-80.
104. Lim, I. I. S.; Mott, D.; Ip, W.; Njoki, P. N.; Pan, Y.; Zhou, S.; Zhong, C.-J., Interparticle Interactions in Glutathione Mediated Assembly of Gold Nanoparticles. *Langmuir* **2008,** *24* (16), 8857-8863.
105. Wells, B., Colloidal gold. Principles methods and applications, vols 1 and 2 M.A. Hayat (ed.). Academic Press, New York. Vol 1 536 pp; Vol 2 484 pp. U.S.$75.00 volume. *Micron and Microscopica Acta* **1990,** *21* (3).
106. Ding, N.; Cao, Q.; Zhao, H.; Yang, Y.; Zeng, L.; He, Y.; Xiang, K.; Wang, G., Colorimetric assay for determination of lead (II) based on its incorporation into gold nanoparticles during their synthesis. *Sensors* **2010,** *10* (12), 11144-11155.
107. Wiegand, H. J.; Ottenwälder, H.; Bolt, H. M., The formation of glutathione-Chromium complexes and their possible role in Chromium disposition. In *Receptors and Other Targets for Toxic Substances*, Chambers, P.; Cholnoky, E.; Chambers, C., Eds. Springer Berlin Heidelberg: 1986; Vol. 8, pp 319-321.
108. Fuhr, B. J.; Rabenstein, D. L., Nuclear magnetic resonance studies of the solution chemistry of metal complexes. IX. Binding of cadmium, zinc, lead, and mercury by glutathione. *Journal of the American Chemical Society* **1973,** *95* (21), 6944-6950.
109. Chen, S.; Fang, Y.-M.; Xiao, Q.; Li, J.; Li, S.-B.; Chen, H.-J.; Sun, J.-J.; Yang, H.-H., Rapid visual detection of aluminium ion using citrate capped gold nanoparticles. *Analyst* **2012,** *137* (9), 2021-2023.
110. Wang, X.; Li, K.; Yang, X. D.; Wang, L. L.; Shen, R. F., Complexation of Al(III) with reduced glutathione in acidic aqueous solutions. *Journal of Inorganic Biochemistry* **2009,** *103* (5), 657-665.

111. Donald J. Pietrzyk; Frank, C. W., *Analytical chemistry*. Academic Press: New York, 1979.
112. Jack Samuel Penciner. Stability constants of metal complexes of 5-sulfosalicylic acid. Toronto Ont University, Toronto, 1962.
113. Cooke, K.; Gould, M. H., The health effects of aluminium--a review. *Journal of the Royal Society of Health* **1991,** *111* (5), 163-8.
114. Buragohain, M.; Bhuyan, B.; Sarma, H. P., Seasonal variations of lead, arsenic, cadmium and aluminium contamination of groundwater in Dhemaji district, Assam, India. *Environmental monitoring and assessment* **2010,** *170* (1-4), 345-51.
115. Stahl, T.; Taschan, H.; Brunn, H., Aluminium content of selected foods and food products. *Environmental Sciences Europe* **2011,** *23* (1), 37.
116. Frankowski, M.; Ziola-Frankowska, A.; Kurzyca, I.; Novotny, K.; Vaculovic, T.; Kanicky, V.; Siepak, M.; Siepak, J., Determination of aluminium in groundwater samples by GF-AAS, ICP-AES, ICP-MS and modelling of inorganic aluminium complexes. *Environmental monitoring and assessment* **2011,** *182* (1-4), 71-84.
117. Chappuis, P.; Poupon, J.; Rousselet, F., A sequential and simple determination of zinc, copper and aluminium in blood samples by inductively coupled plasma atomic emission spectrometry. *Clinica chimica acta; international journal of clinical chemistry* **1992,** *206* (3), 155-65.
118. Jones, P.; Ebdon, L.; Williams, T., Determination of trace amounts of aluminium by ion chromatography with fluorescence detection. *Analyst* **1988,** *113* (4), 641-644.
119. Wang, Z.; Ma, L., Gold nanoparticle probes. *Coordination Chemistry Reviews* **2009,** *253* (11–12), 1607-1618.
120. Li, X.; Wang, J.; Sun, L.; Wang, Z., Gold nanoparticle-based colorimetric assay for selective detection of aluminium cation on living cellular surfaces. *Chemical Communications* **2010,** *46* (6), 988-990.
121. (a) Trojanowicz, M.; Szpunar-Łobińska, J., Simultaneous flow-injection determination of aluminium and zinc using LED photometric detection. *Analytica Chimica Acta* **1990,** *230* (0), 125-130; (b) Shen, H.; Fang, Q., Improved microfluidic chip-based sequential-injection trapped-droplet array liquid-liquid extraction system for determination of aluminium. *Talanta* **2008,** *77* (1), 269-72.

APPENDIX I SUPPORTING INFORMATION FOR CHAPTER III

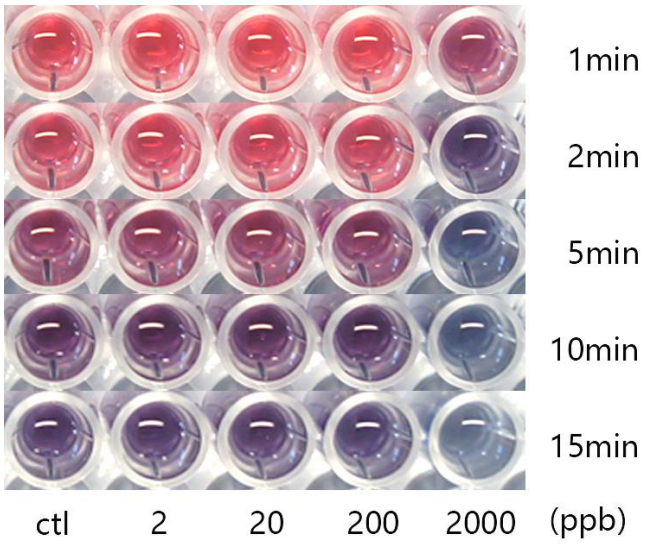

Figure A1: The colour changes of the GNP sensors upon the addition of various amount of lead standard solutions with respect to the time.

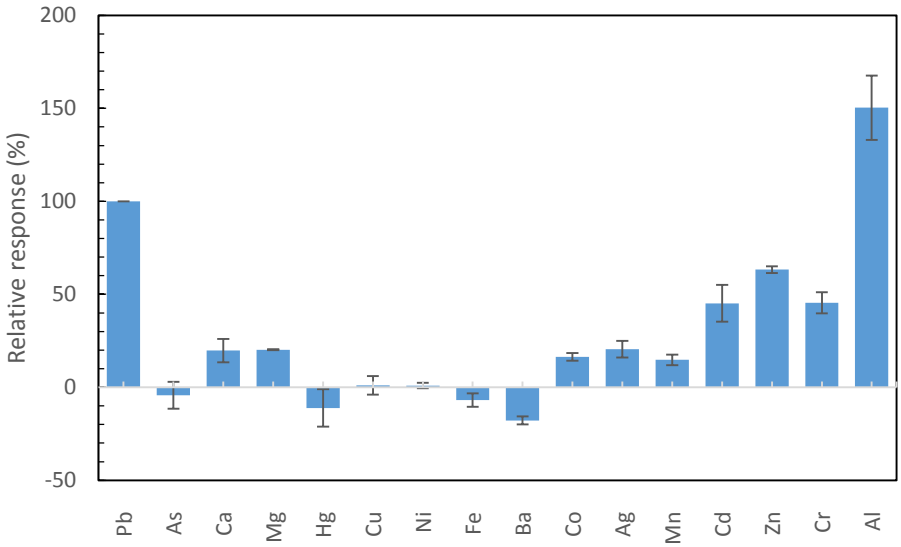

Figure A2: The selectivity test of Pb^{II} in the presence of same concentration (mass basis: 200 ppb) of fourteen metal ions. The value is based on the relative response of the signal intensity of 200 ppb Pb^{II} standard. The concentrations of each ion from As to Al are 2.8, 5.2, 8.5, 1, 3.3, 3.5, 3.7, 1.5, 3.5, 1.9, 3.8, 1.8, 3.2, 4.0, 7.7 μM, respectively.

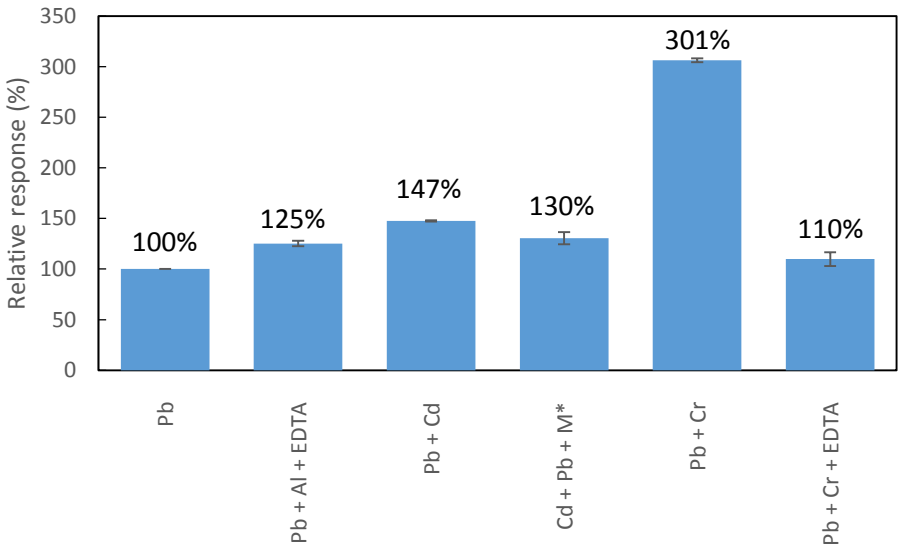

Figure A3: Improvement of the selectivity by the addition of EDTA, NaF and 5-Sulfocylisilic acid as masking agents. Note that each ion was at 200 ppb. *M represents a mixture of NaF and 5-sulfocylisilic acid.